



高效、宽带发射有机-无机金属卤化物荧光材料

赫世辉 赵 静* 刘泉林

(北京科技大学材料科学与工程学院, 北京 100083)

摘要: 有机-无机金属卤化物作为一种新兴的发光材料, 由于其高的发光效率以及宽的发射光谱等优点受到广泛关注。本文以有机-无机金属卤化物高效荧光材料为对象, 根据金属阳离子种类对材料进行归类, 探讨其高效发光机理, 并提出改善该类材料发光效率的方法。总体而言, 对于此类荧光材料的研究还处于起步阶段, 其发光机理仍然存在争议, 本文对当前主流发光机理进行了总结。最后, 对于有机-无机金属卤化物荧光材料的发展前景进行了展望, 旨在进一步推动该类材料在荧光转换发光二极管等领域的应用。

关键词: 金属卤化物; 杂化材料; 宽带发射; 荧光材料

中图分类号: TQ174 文献标识码: A 文章编号: 1001-4861(2022)07-1209-17

DOI: 10.11862/CJIC.2022.107

High-Efficiency and Broad-Spectrum Emitting Organic-Inorganic Metal Halide Photoluminescent Materials

HE Shi-Hui ZHAO Jing* LIU Quan-Lin

(College of Materials Science and Engineering, University of Science and Technology Beijing, Beijing 100083, China)

Abstract: Organic - inorganic metal halides, as an emerging photoluminescent material, have received extensive attention due to their high photoluminescence quantum yield and broad-spectrum emission. This paper focuses on organic-inorganic metal halide high-efficiency photoluminescent materials, classifies the materials according to the types of metal cations, discusses their high-efficiency luminescent mechanism, and proposes methods to improve the luminous efficiency of such materials. In general, the research on such photoluminescent materials is still in its infancy, its light-emitting mechanism is still controversial, and current mainstream light-emitting mechanisms are summarized. Finally, the development prospects of organic-inorganic metal halide photoluminescent materials are prospected, aiming to further promote the application of this type of material in the field of phosphor-converted light-emitting diodes.

Keywords: metal halide; hybrid material; broad-spectrum emission; photoluminescent material

0 引言

有机-无机金属卤化物(OIMHs)半导体材料是目前研究的热点, 其作为发光材料、太阳能电池材

料、非线性光学材料、辐射探测器材料等在光电领域有着广泛的应用前景^[1]。目前, 照明及显示背光源主要是蓝光二极管(LED)结合荧光粉产生所需要的光色。现在应用的荧光粉中都需要引入稀土元

收稿日期: 2021-12-08。收修改稿日期: 2022-03-24。

国家自然科学基金(No.51972021, 52073003)资助。

*通信联系人。E-mail:jingzhao@ustb.edu.cn

素作为发光中心,为了减少对稀土元素的依赖,OIMHs凭借其优异的发光性能,成为当前发光领域研究的关注点。OIMHs的优越性主要体现在高的发光量子效率(PLQY)^[2]和宽谱发射^[3]两方面。OIMHs是实现单一组分白光发射LED的有力候选材料,通过组分调控可实现单一组分发射光谱覆盖整个可见光区^[4]。其成功应用将解决多组分荧光粉在照明中由于自吸收引起的效率降低,以及随使用时间推移,降解速率不同所导致的光色偏差问题。

OIMHs与杂化钙钛矿材料联系紧密,三维(3D)钙钛矿结构中八面体高度有序,结构刚性强。3D钙钛矿结构的通式为ABX₃,其中A是甲基铵(MA)、甲脒(FA)或铯(Cs),B是Pb²⁺、Sb³⁺、Sn²⁺、Bi³⁺等金属离子,X是一种或多种卤化物(Cl、Br或I),它由无限[BX₆]⁴⁻八面体通过角共享和A位阳离子占据的空隙空间构成的3D框架。形成的3D钙钛矿结构是直接带隙半导体,在其中价带最大值(VBM)的特定反键特性和导带最小值(CBM)中的自旋轨道效应仅形成封闭在导带或价带中的浅陷阱^[5]。由于晶格常数的改变,FA大于MA,MA又大于Cs,A位阳离子的选择改变了带隙,导致从FA到MA再到Cs的带隙增加^[1,5]。随着有机物阳离子的增加,带隙也会相应地增加。因此,3D钙钛矿结构中带隙很窄且不存在自陷态激子(STE),使其无法形成宽带发射。目前报道的化合物CsPbX₃(X=Cl、Br或I)钙钛矿纳米晶,PLQY最高可达90%,但是均为窄带发射,其半峰宽最高为35 nm^[6]。MAPbX₃(X=Cl、Br或I)也为窄带发射^[7]。

OIMHs与传统钙钛矿结构ABX₃的最大区别在于A位阳离子不再是简单的无机或小体积有机阳离子^[8],而是换成了大的有机阳离子(C₉NH₂₀⁺、C₇NH₉⁺等)^[9];B位的金属阳离子包括最外层具有不同电子

组态的+1、+2、+3、+4价离子;X位为卤素离子。值得注意的是,低维度的OIMHs中B位和X位结合形成的多面体,不再局限于八面体结构,还有三面体、四面体、跷跷板、金字塔以及多核聚集体等结构。

本文首先按照金属阳离子的最外层电子层分布将OIMHs发光材料分为3类(ns^2 、 d^{10} 、 d^5)。然后,讨论OIMHs发光机理,包括STE发光、 ns^2 孤立中心发光、Mn²⁺孤立中心发光以及混合机理。最后,重点讨论了提高OIMHs的PLQY的方法并对该系列化合物的发展前景进行了展望。

1 高效发光OIMHs材料的分类

1.1 ns^2 系列

含有 ns^2 电子的阳离子包括Pb²⁺、Bi³⁺、Sn²⁺、Sb³⁺等。 ns^2 离子在光激发过程中表现出 ns^2 孤对电子跃迁特性。

1.1.1 $6s^2$ 系列

$6s^2$ 系列金属阳离子中包括Pb²⁺和Bi³⁺等,该系列杂化金属卤化物的发光主要来自无机基团,其中孤对电子会引起激发态结构畸变,降低激子的运输能力。使运输过程中造成的复合减弱,相应的非辐射跃迁就会降低,其PLQY则会增加^[10]。但是受限于畸变程度较低,导致其PLQY整体不高。通常通过掺杂或者形成多聚体发光中心的形式来调整结构,进而提高其PLQY。

Ma课题组^[11]较早合成了高PLQY的C₄N₂H₁₄PbBr₄,其晶体结构如图1a所示。该化合物为一维(1D)结构,2个八面体通过共边连接形成双八面体链,其单晶在紫外灯照射下呈现蓝白光,PLQY约20%。另外,Zhang课题组报道了(2cepiH)PbBr₃^[12],如图1b所示,其由共面PbBr₆⁴⁻八面体组成1D无限[PbBr₃]ⁿ⁻链

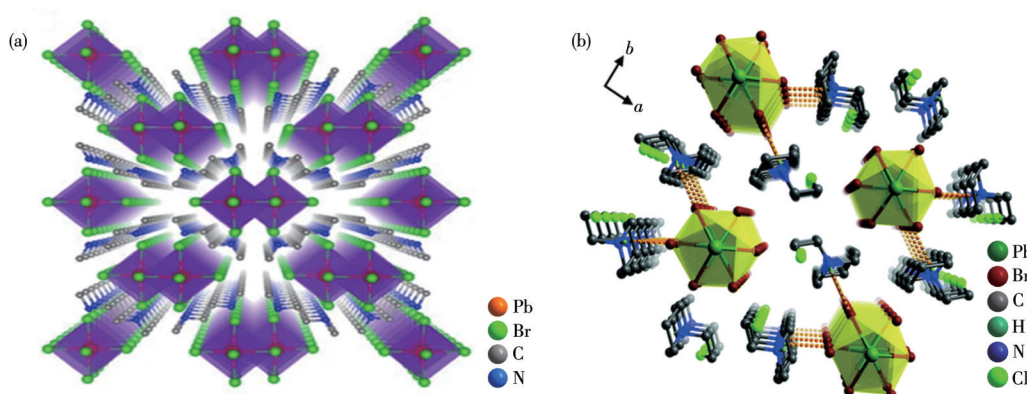


图1 (a) C₄N₂H₁₄PbBr₄^[11]和(b) (2cepiH)PbBr₃^[12]的晶体结构
Fig.1 Crystal structures of (a) C₄N₂H₁₄PbBr₄^[11] and (b) (2cepiH)PbBr₃^[12]

状结构,其PLQY为16.8%。其它Pb²⁺基的高效荧光材料如表1所示。Bi³⁺基的OIMHs研究很少^[13-16],其存在形式主要是八面体[BiX₆]³⁻,目前报道的化合物的PLQY都很低,即使形成二聚体^[17-18][Bi₂X₉]³⁻、

[Bi₂X₁₀]⁴⁻、[Bi₂X₁₁]⁵⁻,PLQY仍然很低。因此,对于追求高效发光材料而言,以Bi³⁺作为中心阳离子的化合物有待进一步研究。

表1 6s²系列OIMHs的无机结构单元和主要发光性质参数Table 1 Inorganic unit structure and main luminescent property parameters of 6s² series OIMHs*

Inorganic unit structure	Compound	Abbr.	λ_{em} / nm	PLQY	Ref.
[PbX ₄] ²⁻ (X=Cl, Br)	C ₄ N ₂ H ₁₄ PbBr ₄	—	475	20%	[11]
	(2cepiH)PbBr ₃	2cepi	583	16.8%	[12]
	(EDBE)[PbBr ₄]	EDBE	573	9%	[19]
	Bmpip ₂ PbBr ₄	Bmpip	520	24%	[20]
	[PP14] ₂ [PbBr ₄]	PP14	470	28.21%	[21]
	(C ₁₃ H ₁₉ N ₄) ₂ PbBr ₄	—	460	40%	[22]
	(C ₈ NH ₁₂) ₂ PbBr ₄	—	426	15%	[23]
	(C ₄ H ₉ NH ₃) ₂ PbBr ₄	—	406	26%	[24]
[PbX ₆] ⁴⁻ (X=Cl, Br)	(C ₃ N ₃ H ₁₁ O) ₂ PbBr ₆ ·4H ₂ O	—	568	9.6%	[25]
	C ₅ H ₁₆ N ₂ Pb ₂ Br ₆	—	550	10%	[26]
	[H ₂ BPP]Pb ₂ Br ₆	BPP	524	8.1%	[27]
	[DTHPE] _{0.5} PbCl ₃	DTHPE	458	6.99%	[28]
	TMHDAPb ₂ Br ₆	TMHDA	565	12.8%	[29]
	(C ₂₀ H ₁₈ N ₂)(Pb ₃ Cl ₈)	—	682	6.4%	[30]
	(TDMP)PbBr ₄	TDMP	372	45%	[31]
	(2,6-dmpz) ₃ Pb ₂ Br ₁₀	2,6-dmpz	585	12%	[9]
	(C ₉ NH ₂₀) ₆ Pb ₃ Br ₁₂	—	522	12%	[32]

*Abbr.: abbreviation; 2cepi=1-(2-chloroethyl)-piperidine; EDBE=2,2'-(ethylenedioxy)bis(ethylamine); Bmpip=1-butyl-1-methylpiperidinium; PP14=N-butyl-N-methylpiperidinium; BPP=1,3-bis(4-pyridyl)-propane; DTHPE=C₁₀N₄H₁₈; TMHDA=N,N,N',N'-tetramethyl-1,6-hexanediammonium; TDMP=trans-2,5-dimethylpiperazine; 2,6-dmpz=2,6-dimethylpiperazine; λ_{em} : position of emission peak.

1.1.2 5s²系列

含有5s²孤对电子的金属阳离子有Sn²⁺、Sb³⁺和Te⁴⁺,虽然5s²和6s²杂化金属卤化物的基态电子结构相似,但是其孤对电子的立体活性和结构可调性都比6s²更好,其中化学活性较高的Sn²⁺孤对电子导致该系列化合物激发态结构畸变更强,斯托克斯(Stokes)位移更大。大的Stokes位移可以减少激发和发射之间的光谱重叠,从而限制了激发能的共振传递。如果不满足谐振条件,激子转移需要声子辅助,从而显著降低能量传输效率。激子迁移的抑制降低了激子遇到缺陷的概率,从而降低了非辐射复合率,提高了光致PLQY。温度的升高使激发和发射带变宽^[10,33-34]。

Fan课题组^[35]合成的(C₁₀H₂₈N₄Cl₂)SnCl₄·2H₂O的PLQY高达92.3%,其中Sn²⁺形成四面体结构[SnCl₄]²⁻(图2a)。Ma课题组^[36]合成出化合物(C₄N₂H₁₄Br)₄SnBr₆,其中Sn²⁺形成八面体配位结构[SnBr₆]⁴⁻,其PLQY接

近100%(图2b)。这些研究结果说明Sn²⁺替代Pb²⁺在降低材料毒性的同时有效提高了PLQY,但是Sn²⁺稳定性较低,易被氧化为Sn⁴⁺,制约了其进一步发展。相较而言,Sb³⁺的稳定性更高,其主要结构为金字塔型[SbX₅]²⁻和八面体型[SbX₆]³⁻。统计发现,含有[SbX₅]²⁻的OIMHs的PLQY更高一些(表2)。Ma课题组^[36]合成出(C₉NH₂₀)₂SbCl₅,其在紫外灯下呈现黄色,PLQY接近于100%(图2c)。关于Te⁴⁺的研究较少,其主要是以八面体[TeX₆]⁴⁻形式存在。Kundu课题组^[37]报道了(BzTEA)₂TeCl₆,其在紫外灯下呈现橙色,PLQY为15%(图2d)。总体而言,5s²体系PLQY较高,是研究高效发光材料的重点。

1.2 d¹⁰系列

d¹⁰系列金属阳离子也是OIMHs发光材料研究的重点,包括Ag⁺、Cu⁺、Cd²⁺、Zn²⁺、In³⁺、Sn⁴⁺等。

其中,研究较多的是In³⁺、Zn²⁺和Cu⁺。In³⁺存在八面体[InX₆]³⁻和四面体[InX₄]⁻两种配位形式。

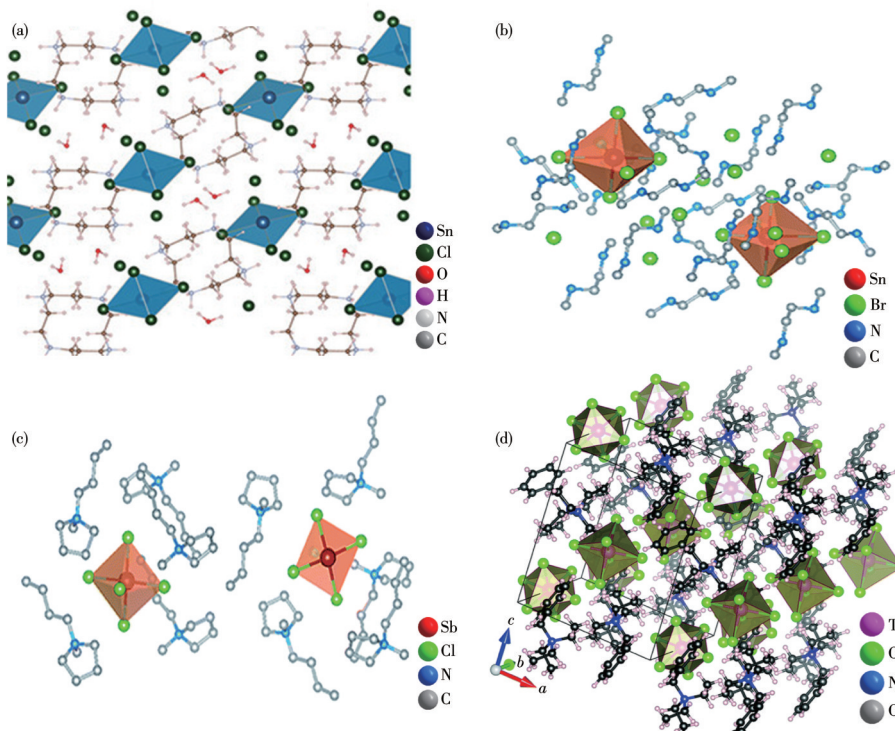


图2 (a) $(C_{10}H_{28}N_4Cl_2)SnCl_4 \cdot 2H_2O^{[35]}$ 、(b) $(C_4N_2H_{14}Br)_4SnBr_6^{[36]}$ 、(c) $(C_9NH_{20})_2SbCl_5^{[36]}$ 和(d) $(BzTEA)_2TeCl_6^{[37]}$ 的晶体结构
Fig.2 Crystal structures of (a) $(C_{10}H_{28}N_4Cl_2)SnCl_4 \cdot 2H_2O^{[35]}$, (b) $(C_4N_2H_{14}Br)_4SnBr_6^{[36]}$, (c) $(C_9NH_{20})_2SbCl_5^{[36]}$, and (d) $(BzTEA)_2TeCl_6^{[37]}$

表2 5s²系列OIMHs的无机结构单元和主要发光性质参数

Table 2 Inorganic unit structure and main luminescent property parameters of 5s² series OIMHs

Inorganic unit structure	Compound	Abbr.*	λ_{em} / nm	PLQY	Ref.
$[SnX_4]^{2-}$ (X=Cl, Br, I)	Bmpip ₂ SnBr ₄	Bmpip	665	75%	[20]
	(OCTAm) ₂ SnBr ₄	OCTAm	600	95%±5%	[38]
	(OCTAm) ₂ SnI ₄	OCTAm	670	41%	[38]
	$(C_{10}H_{28}N_4Cl_2)SnCl_4 \cdot 2H_2O$	—	639	92.3%	[35]
$[SnX_6]^{4-}$ (X=Cl, Br, I)	$(C_{10}H_{28}N_4)SnBr_6 \cdot 4H_2O$	—	530	61.7%	[35]
	$(C_4N_2H_{14}Br)_4SnBr_6$	—	570	95%±5%	[36]
	$(C_4N_2H_{14}I)_4SnI_6$	—	620	75%±4%	[36]
	$(C_6H_{18}N_2)_3SnBr_8$	—	601	86%±2%	[39]
	ODASnBr ₄	ODA	570-608	83%±4%	[40]
	$(C_8H_{14}N_2)_2SnBr_6$	—	507	36%±4%	[41]
	$[BMIm][Sn(AlCl_4)_3]$	BMIm	448	51%	[42]
	$[BMPyr][Sn(AlCl_4)_3]$	BMPyr	453	76%	[42]
$[SbX_5]^{2-}$ (X=Cl, Br)	$(C_9NH_{20})_2SbCl_5$	—	590	98%±2%	[36]
	$(Ph_4P)_2SbCl_5$	Ph ₄ P	648	87%	[43]
	$(TTA)_2SbCl_5$	TTA	625	68%	[44]
	$(TEBA)_2SbCl_5$	TEBA	590	72%	[44]
	TPP_2SbBr_5	TPP	682	33%	[45]
	$(PPN)_2SbCl_5$	PPN	635	98.1%	[46]
$[TeX_6]^{2-}$ (X=Cl, Br)	$(BzTEA)_2TeCl_6$	BzTEA	610	15%	[37]

*OCTAm=n-Octylamine; ODA=1,8-octanediamine; BMIm=1-butyl-3-methylimidazolium; BMPyr=1-butyl-1-methyl-pyrrolidinium;

Ph₄P=tetraphenylphosphonium; TTA=tetraethylammonium; TEBA=benzyltriethylammonium; TPP=tetraphenylphosphonium; PPN=bis(triphenylphosphoranylidene)ammonium; BzTEA=benzyltriethylammonium.

(PMA)₃InBr₆具有0D结构,含有[InBr₆]³⁻八面体,PLQY为35%,其发射光颜色为橙色(图3a)^[47]。RInBr₄含有孤立的[InBr₄]⁻四面体,PLQY为16.36%,其发射光颜色为蓝色(图3b)^[48]。Zn²⁺多以四面体结构[ZnX₄]²⁻形式存在^[49],Ma课题组^[50]合成的TPP₂ZnCl₄具有优良的长余辉性能,PLQY为28.8%。Tang团队^[51]合成的(C₁₆H₃₆N)CuI₂中含有[Cu₂X₄]²⁻二聚体,PLQY达到54.3%(图3c)。Zhang课题组^[52]合成的Hmta[(Hmta)Ag₄I₄]结构由四面体Ag₄I₄单元和Hmta交替排列组成,PLQY达到18.5%。

对于空气和热稳定性,Sn⁴⁺基材料是Sn²⁺基材料的理想替代品。但是,Sn⁴⁺由于没有立体化学活性

孤对的电子以及[SnX₆]²⁻中几乎没有结构畸变^[8],因此其发光性能较弱,目前已知结构中(C₆N₂H₁₆Cl)₂SnCl₆的效率最高,为8.1%^[53]。当Sn²⁺被氧化成Sn⁴⁺时,其会失去最外层的5s²电子,化学活性降低,相应的激发态结构畸变也会随之减少,Stokes位移减小,相应的激发和发射之间的光谱重叠,增加了激发能的共振传递。激子迁移的增加提高了激子遇到缺陷的概率,从而增加了非辐射复合率,使PLQY降低^[33]。由于没有孤对电子的存在,d¹⁰整体的PLQY相比于5s²系列低一些(表3),对于d¹⁰系列的研究可以通过掺杂等方式来进一步改善其PLQY。

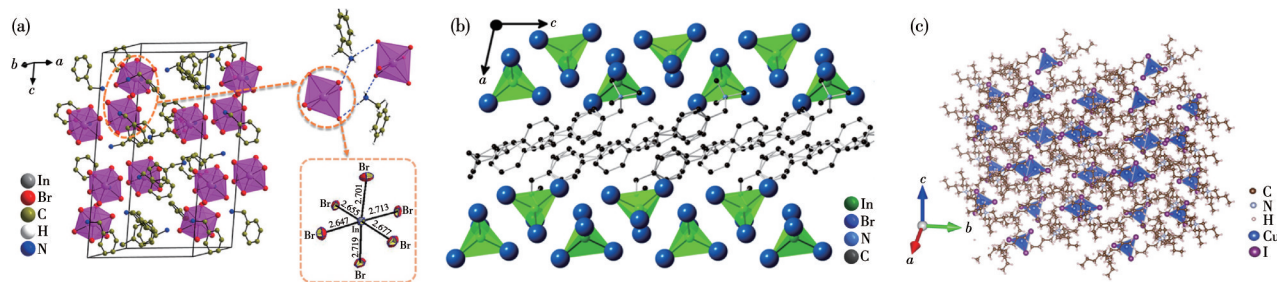


图3 (a) (PMA)₃InBr₆^[47]、(b) RInBr₄^[48]和(c) (C₁₆H₃₆N)CuI₂^[51]的晶体结构
Fig.3 Crystal structures of (a) (PMA)₃InBr₆^[47], (b) RInBr₄^[48], and (c) (C₁₆H₃₆N)CuI₂^[51]

表3 d¹⁰系列OIMHs的无机结构单元和主要发光性质参数

Table 3 Inorganic unit structure and main luminescent property parameters of d¹⁰ series OIMHs

Inorganic unit structure	Compound	Abbr.*	λ_{em} / nm	PLQY	Ref.
[InX ₆] ³⁻ (X=Cl, Br)	(PMA) ₃ InBr ₆	PMA	610	35%	[47]
[InX ₄] ⁻ (X=Cl, Br)	RInBr ₄	R	437	16.36%	[48]
Multimeric form of Cu ⁺	(TBA)CuBr ₂	TBA	511	55%	[54]
	(C ₁₆ H ₃₆ N)CuI ₂	—	476, 675	54.3%	[51]
	(DTA) ₂ Cu ₂ I ₄	DTA	540	60%	[55]
	(Gua) ₃ Cu ₂ I ₅	Gua	481	96%	[56]
	(18-crown-6) ₂ Na ₂ (H ₂ O) ₃ Cu ₄ I ₆	18-crown-6	536	91%	[57]
	Cu ₂ I ₂ (Ph ₃ P) ₂	Ph ₃ P	595	19%	[58]
	Cu ₄ I ₄ (P(C ₆ H ₄ —OCH ₃) ₃) ₄	—	558	72%	[59]
	Cu ₄ I ₄ (P(C ₆ H ₄ —CH ₃) ₃) ₄	—	515	50%	[59]
	Cu ₄ I ₄ (P(C ₆ H ₅) ₃) ₄	—	525	88%	[59]
	[Cu ₄ I ₄ (PPh ₂ (C ₆ H ₄ CH ₂ OH)) ₄]·CH ₃ CN	PPh ₂ (C ₆ H ₄ CH ₂ OH)	542	73%	[60]
	[Cu ₄ I ₄ (PPh ₂ (C ₆ H ₄ CH ₂ OH)) ₄]·3C ₄ H ₈ O	PPh ₂ (C ₆ H ₄ CH ₂ OH)	540	55%	[60]
	Cu ₄ I ₄ (PPh ₂ Pr) ₄	PPh ₂ Pr	560	60%	[61]
[ZnX ₄] ²⁻ (X=Cl, Br)	(C ₂₀ H ₁₈ N ₂)(ZnCl ₄)	—	595	31.31%	[30]
	TPP ₂ ZnCl ₄	TPP	353	28.8%	[50]
	(C ₅ H ₇ N ₂) ₂ ZnBr ₄	—	420	19.18%	[62]
	[(N-AEPz)ZnCl ₄]Cl	N-AEPz	550	11.52%	[63]
[HgX ₄] ²⁻ (X=Cl, Br)	(C ₅ H ₇ N ₂) ₂ HgBr ₄	—	560	14.87%	[62]
[CdX ₄] ²⁻ (X=Cl, Br)	(C ₂₀ H ₁₈ N ₂)(CdCl ₄)	—	583	46.89%	[30]

续表3

Multimeric form of Ag^+	$\text{Ag}_2\text{I}_2(1,5\text{-naphthyridine})$	—	566	15%	[58]
	$\text{Hmta}[(\text{Hmta})\text{Ag}_4\text{I}_4]$	Hmta	620	18.5%	[52]
	$[\text{HDABCO}]_3\text{Ag}_5\text{Cl}_8$	DABCO	585	6.7%	[64]
$[\text{SnX}_6]^{2-}$ ($\text{X}=\text{Cl}, \text{Br}$)	$(\text{C}_6\text{N}_{12}\text{H}_{16}\text{Cl}_6)_2\text{SnCl}_6$	—	450	8.1%	[53]

*PMA=phenylmethylammonium; R=trimethyl(4-stilbenyl)methylammonium; TBA=tetrabutylammonium; DTA=dodecyl trimethyl ammonium; Gua=guanidine; 18-crown-6= $\text{C}_{12}\text{H}_{24}\text{O}_6$; Ph_3P =triphenylphosphine; $\text{PPh}_2(\text{C}_6\text{H}_4\text{CH}_2\text{OH})$ =4-(diphenylphosphino)phenylmethanol; PPh_2Pr =diphenylpropylphosphine; N-AEPz= N -aminoethylpiperazine; Hmta=hexamethylenetetramine; DABCO=1,4-diazabicyclo[2.2.2]octane.

1.3 d^5 系列

d^5 系列中,主要的研究对象是 Mn^{2+} ,其形成的配位多面体主要是四面体 $[\text{MnX}_4]^{2-}$ 和八面体 $[\text{MnX}_6]^{4-}$,还有少部分会形成三聚体结构 $[\text{Mn}_3\text{X}_{12}]^{6-}$ 。

目前合成的OIMHs中, Mn^{2+} 形成四面体结构的居多,其在紫外灯光下呈现出绿光发射。Gong等^[65]报道了2种化合物 $[\text{P}14]_2[\text{MnBr}_4]$ 和 $[\text{PP}14]_2[\text{MnBr}_4]$ (图4a、4b)。其中,前者的PLQY为81%,后者的PLQY为55%。 $[\text{P}14]_2[\text{MnBr}_4]$ 中的 $[\text{MnBr}_4]^{2-}$ 是完全有序的,

$[\text{PP}14]_2[\text{MnBr}_4]$ 中的 $[\text{MnBr}_4]^{2-}$ 是无序的,四面体结构的有序性对于PLQY有很大的影响。六配位的 Mn^{2+} 在紫外灯光下呈现出红光发射。Zou团队^[66]合成的 $(\text{CH}_6\text{N}_3)_2\text{MnCl}_4$ 表现出强烈的红光发射,其PLQY为55.9%(图4c)。其它 Mn 基高效发光的化合物见表4。 Mn 可以作为中心金属阳离子存在于OIMHs的晶格中,还可作为掺杂剂的形式存在,使其在高效OIMHs的研究中所占的比重日益增加。

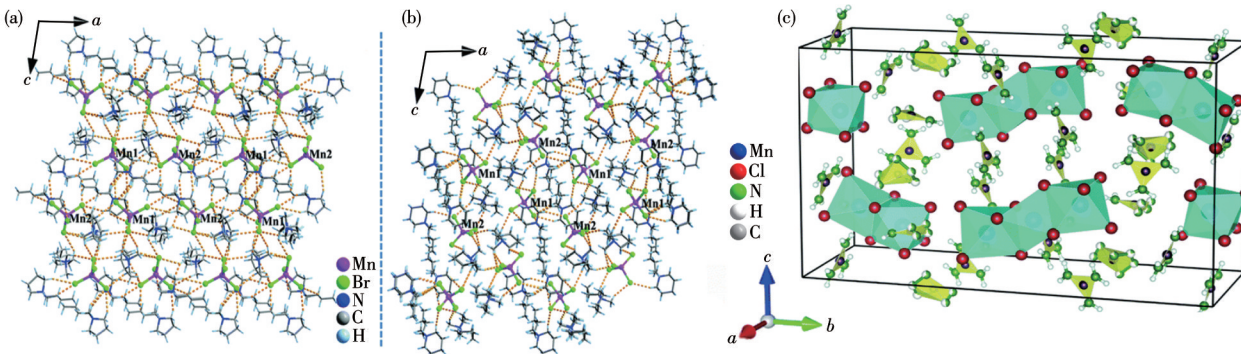


图4 (a) $[\text{P}14]_2[\text{MnBr}_4]$ 、(b) $[\text{PP}14]_2[\text{MnBr}_4]$ ^[65]和(c) $(\text{CH}_6\text{N}_3)_2\text{MnCl}_4$ ^[66]的晶体结构
Fig.4 Crystal structure of (a) $[\text{P}14]_2[\text{MnBr}_4]$, (b) $[\text{PP}14]_2[\text{MnBr}_4]$ ^[65], and (c) $(\text{CH}_6\text{N}_3)_2\text{MnCl}_4$ ^[66]

表4 Mn系列OIMHs的无机单元结构和主要发光性质参数

Table 4 Inorganic unit structure and main luminescent property parameters of Mn series OIMHs

Inorganic unit structure	Compound	Abbr.*	$\lambda_{\text{em}} / \text{nm}$	PLQY	Ref.
$[\text{MnX}_4]^{2-}$ ($\text{X}=\text{Cl}, \text{Br}, \text{I}$)	$[\text{P}_{14}]_2[\text{MnBr}_4]$	P14	520	81%	[65]
	$[\text{PP}_{14}]_2[\text{MnBr}_4]$	PP14	527	55%	[65]
	$[\text{Bu}_4\text{N}]_2[\text{MnBr}_4]$	Bu ₄ N	520	47%	[67]
	$[\text{Ph}_3\text{P}]_2[\text{MnBr}_4]$	Ph ₃ P	520	47%	[67]
	$[\text{C}_9\text{NH}_{20}]_2[\text{MnBr}_4]$	—	528	81.08%	[68]
	$[\text{C}_7\text{H}_{10}\text{N}]_2[\text{MnCl}_4]$	—	523	82%	[69]
	$[\text{C}16\text{Py}]_2[\text{MnBr}_4]$	C16Py	540	65%	[70]
	$[\text{C}16\text{mim}]_2[\text{MnBr}_4]$	C16mim	530	61%	[70]
	$(\text{C}_{20}\text{H}_{20}\text{P})_2\text{MnBr}_4$	—	523	93.83%	[71]
	$(\text{TMPEA})_2\text{MnBr}_4$	TMPEA	520	98%	[72]
	$(\text{BTMA})_2\text{MnBr}_4$	BTMA	519	72%	[72]
	$(\text{Bz}(\text{Me})_3\text{N})_2\text{MnCl}_4$	Bz(Me) ₃ N	547	78%	[73]
	$(\text{Bz}(\text{Me})_3\text{N})_2\text{MnBr}_4$	Bz(Me) ₃ N	516	63%	[73]

续表4

$(n\text{-PrBrMe}_3\text{N})_2\text{MnCl}_4$	$n\text{-PrBrMe}_3\text{N}$	512	81%	[73]
$(\text{KC})_2\text{MnBr}_4$	KC	520	38.5%	[74]
$(\text{C}_4\text{NOH}_{10})_2\text{MnCl}_4$	—	450	39%	[75]
$(1\text{-C}_5\text{H}_{14}\text{N}_2\text{Br})_2\text{MnBr}_4$	—	520	60.7%	[76]
$(\text{C}_4\text{H}_9\text{NH}_3)_2\text{MnI}_4$	—	550, 672	68%	[77]
$[\text{MnX}_6]^{4-}$ ($\text{X}=\text{Cl}, \text{Br}, \text{I}$)	(Pyrrolidinium) MnCl_3	—	640	56%
	(3-Pyrrolinium) MnCl_3	—	635	28%
	$(\text{C}_4\text{NOH}_{10})_5\text{Mn}_2\text{Cl}_9 \cdot \text{C}_2\text{H}_5\text{OH}$	—	620	29%
	$(\text{CH}_6\text{N}_3)_2\text{MnCl}_4$	—	650	55.9%
				[66]

*P14=N-butyl-N-methylpyrrolidinium; Bu_4N =tetrabutylammonium; C16Py=cetylpyridinium; C16mim=1-methyl-3-hexadecylimidazolium; TMPEA=trimethylphenylammonium; BTMA=benzyltrimethylammonium; Bz(Me)₃N=N-benzyl-N,N,N-trimethyl; KC=K(dibenzo-18-crown-6).

1.4 含有多个B位阳离子的OIMHs

研究表明在单一金属阳离子OIMHs的基础上,通过引入另外的金属阳离子,形成多中心金属阳离子OIMHs,可以进一步扩展发射光谱的宽度实现单一组分白光发射。Ma课题组^[80]合成的 $(\text{HMTA})_4\text{PbMn}_{0.69}\text{Sn}_{0.31}\text{Br}_8$ 包括了 PbBr_4^{2-} 、 MnBr_4^{2-} 、 SnBr_4^{2-} 单体结构,实现了白光发射,其PLQY达到73%(图5a和5b)。多中心金属阳离子化合物的另外一种存在方式就是多聚体和单体结构结合,多聚体研究中以 $[\text{Pb}_3\text{X}_{11}]^{5-}$ 三聚体研究最多,它是由3个 $[\text{PbX}_6]^{4-}$ 八面体通过共面连接形成的,结构中引入另外一种金属离子的单体结构进行光谱调控,形成不同颜色的光,多个阳离子中心同时也会使材料PLQY得到极大的提高(表5)。例如Xia课题组^[81]报道的 $(\text{C}_9\text{NH}_{20})_9\text{Pb}_3\text{X}_{11}(\text{MX}_4)_2$ ($\text{X}=\text{Br}$ 、

Cl ; $\text{M}=\text{Mn}、\text{Fe}、\text{Co}、\text{Ni}、\text{Cu}$ 和 Zn)系列化合物,其呈现出不同颜色的发光且PLQY也不尽相同(图5c~5e)。其它多中心金属阳离子化合物见表5,多中心金属阳离子化合物的合成和研究正在逐渐成为调整发光谱图和提高PLQY的有效措施。

2 OIMHs的发光机理

目前,有关OIMHs的研究在不断增加,其发光本质也逐渐被揭示。已报道的发光机理主要包括STE、 ns^2 孤对电子、 Mn^{2+} 孤立中心发光以及混合机理发光。

2.1 STE发光

STE发光是目前解释具有低晶体结构维度的OIMHs发光的主流机理(图6)。STE的产生是由于

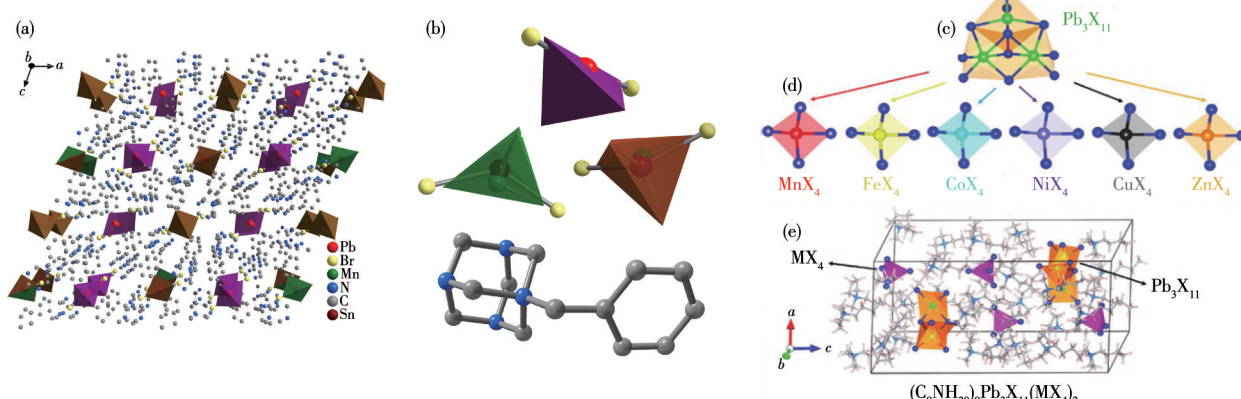


图5 (a) $(\text{HMTA})_4\text{PbMn}_{0.69}\text{Sn}_{0.31}\text{Br}_8$ 的单晶结构;(b)结构单元: PbBr_4^{2-} (紫色四面体)、 MnBr_4^{2-} (绿色四面体)、 SnBr_4^{2-} (棕色四面体)和有机阳离子 HAMT^+ ^[80];(c)提出 $(\text{C}_9\text{NH}_{20})_9\text{Pb}_3\text{X}_{11}(\text{MX}_4)_2$ 的结构设计原理,突出 $[\text{Pb}_3\text{X}_{11}]^{5-}$ 三聚体的局部结构;(d)具有不同M位阳离子的 $[\text{MX}_4]^{2-}$;(e) $(\text{C}_9\text{NH}_{20})_9\text{Pb}_3\text{X}_{11}(\text{MX}_4)_2$ 的晶胞^[81]

Fig.5 (a) Single-crystal structure of $(\text{HMTA})_4\text{PbMn}_{0.69}\text{Sn}_{0.31}\text{Br}_8$; (b) Building blocks: PbBr_4^{2-} (purple tetrahedron), MnBr_4^{2-} (green tetrahedron), SnBr_4^{2-} (brown tetrahedron), and the organic cation HAMT^+ ^[80]; (c) Proposed structural design principle of $(\text{C}_9\text{NH}_{20})_9\text{Pb}_3\text{X}_{11}(\text{MX}_4)_2$ highlighting the local structure of $[\text{Pb}_3\text{X}_{11}]^{5-}$ block; (d) $[\text{MX}_4]^{2-}$ block with different M-position cations; (e) Unit cell of $(\text{C}_9\text{NH}_{20})_9\text{Pb}_3\text{X}_{11}(\text{MX}_4)_2$ ^[81]

表5 多中心金属阳离子OIMHs的无机单元结构和主要发光性质参数

Table 5 Inorganic unit structure and main luminescent property parameters of multi-component OIMHs

Compound	Abbr.*	λ_{em} / nm	PLQY	Ref.
(C ₉ NH ₂₀) ₉ [Pb ₃ Cl ₁₁](ZnCl ₄) ₂	—	516	90.8%	[81]
(C ₉ NH ₂₀) ₉ [Pb ₃ Cl ₁₁](MnCl ₄) ₂	—	519	83.3%	[81]
(bmPy) ₉ [SbCl ₅] ₂ [Pb ₃ Cl ₁₁]	bmPy	516, 673	>70%	[82]
(bmPy) ₉ [ZnBr ₄] ₂ [Pb ₃ Br ₁₁]	bmPy	564	7%	[83]
(bmPy) ₉ [ZnCl ₄] ₂ [Pb ₃ Cl ₁₁]	bmPy	512	ca. 100%	[84]
(C ₉ NH ₂₀) ₉ [Pb ₃ Br ₁₁](MnBr ₄) ₂	—	528, 565	49.8%	[85]
(C ₉ NH ₂₀) ₇ [PbCl ₄] ₂ [Pb ₃ Cl ₁₁]	—	470	83%	[86]
(Emim) ₈ [SbCl ₆] ₂ [SbCl ₅]	Emim	577	11.2%	[87]
[PP14] ₉ [Pb ₃ Br ₁₁][PbBr ₄] ₂	PP14	500	9.54%	[21]
(Bmpip) ₂ Pb _{0.16} Sn _{0.84} Br ₄	Bmpip	470, 670	39%	[88]
(HMTA) ₄ PbMn _{0.69} Sn _{0.31} Br ₈	HMTA	460, 550, 650	73%	[80]
(C ₅ H ₁₄ N ₂) ₂ Pb ₄ MnCl ₁₄	—	678	32%	[89]

*bmPy=1-butyl-1-methylpyrrolidinium; Emim=1-ethyl-3-methylimidazolium; HMTA=N-benzylhexamethylenetetramine.

激子-声子的强耦合,使激发态晶格产生了瞬态的弹性畸变,造成了自由激子(FE)的俘获,也被称为本征STE^[90]。STE可以通过辐射跃迁的方式释放出能量。当能量增加时,STE也可以向FE进行转换^[91]。STE参与的光发射的表现是宽带发射且斯克托斯位移较大。材料处于基态时这种产生STE的瞬态畸变消失,它不同于永久缺陷。永久缺陷有时也会与FE相互耦合,促进STE的形成,也被称为非本征STE。缺陷可能会从稳态吸收光谱中表现出亚带隙吸收,而STE没有从稳态吸收中表现出吸收信号^[92]。此外,从瞬态吸收来看,缺陷会表现出负的亚带隙漂白信号,而STE则表现出正的吸收信号^[93]。此外,从激励功率相关的光致发光(PL)测量结果来看,当由

永久缺陷主导宽带发射时,预期会出现饱和PL。相反,如果宽带发射来自STE,则激励功率与PL呈线性关系,不会出现饱和的PL现象^[19,25,90,94]。

由于晶格变形和载流子-声子耦合,基于STE的稳态光谱通常表现出较大的Stokes位移和宽谱发射;在低温光谱中,可以看到化合物随着温度升高会出现展宽的现象;在寿命光谱中,其从激发态跃迁回基态的时间更长。在瞬态光谱中,STE的光诱导信号(PIA)比FE的PIA达到峰值所需要的时间更长,衰减弛豫时间也更长^[92]。

2.2 ns^2 孤对电子发光

目前,对于 ns^2 系列合成的化合物,主要使用的模型有3种:(1)如图7a所示,自由 ns^2 离子的能级图

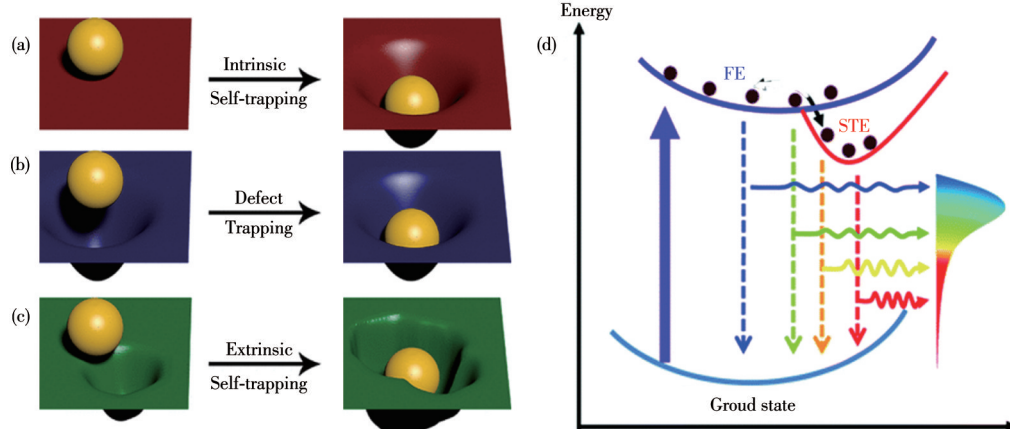


图6 (a) 自捕获、(b) 永久缺陷的捕获和(c) 受永久缺陷影响的自捕获^[90]; (d) STE 和 FE 的发射机理图^[91]

Fig.6 (a) Self-trapping, (b) trapping at permanent defects, and (c) self-trapping influenced by permanent defects^[90];

(d) Emission mechanism diagram of STE and FE^[91]

中,其基态用 1S_0 表示,当发生库仑和交换相互作用时, $nsnp$ 激发态会分裂为 1P 和 3P ,然后经过自旋轨道耦合, 3P 会分裂为非简并态的 3P_0 、 3P_1 、 3P_2 ;(2)如图7b所示,分子轨道理论中,由于配位场的作用,中心金属和配体之间的电子轨道会发生很大程度的杂

化,进而形分子能级;(3)如图7c所示,在半导体材料中,通常用STE模型来解释 ns^2 发光,激发态结构扭曲程度会影响到达激发态所需能量,进而影响发射。Kovalenko课题组将3个模型进行结合,形成了如图7d所示的统一模型^[10]。

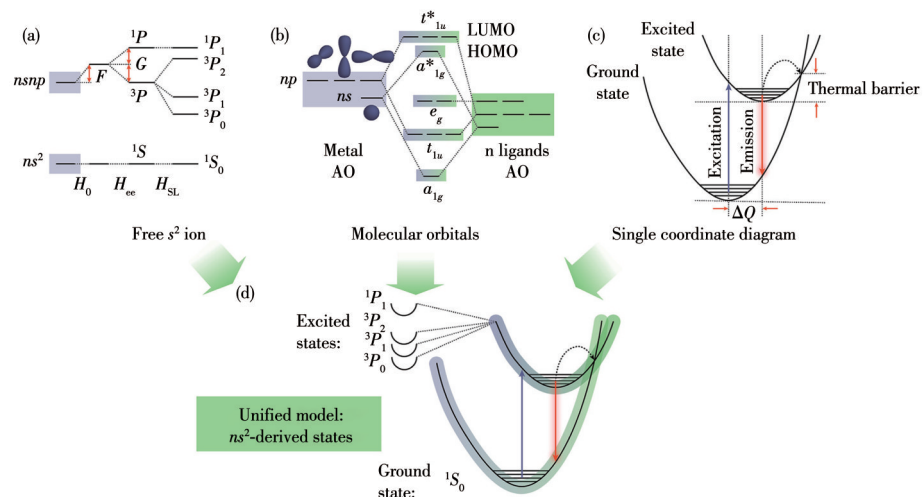


图7 (a) 自由 ns^2 离子的能级图;(b) 金属-卤化物分子轨道图,图中AO表示原子轨道;(c) 简化STE模型在OD 5s²金属卤化物中的位型坐标图;(d) 用位型坐标图表示的统一模型,其中基态和激发态使用其从活性 ns^2 金属离子衍生的原子特性进行描述^[10]

Fig.7 (a) Energy band diagram associated with the free ns^2 ion; (b) Metal-halide molecular orbital diagram where AO represents atomic orbital ; (c) Configurational coordinate diagram of the simplified STE model in OD $5s^2$ metal halides; (d) Unified model with the configurational coordinate diagram, in which the ground and excited states are described using their atomic character as derived from the active ns^2 metal ion^[10]

2.3 Mn²⁺的孤立发光中心

四面体配位的 $[\text{MnX}_4]^{2-}$ 处于弱晶体场,发射绿光;八面体配位的 $[\text{MnX}_6]^{4-}$ 处于强晶体场,发射红光。其发射机理均为 ${}^4T_1 \rightarrow {}^6A_1$ 跃迁(图8a和8b)^[73,95]。对于

Mn²⁺掺杂而言,则是主体化合物吸收激发光,进行能量转移,Mn²⁺作为激活剂,实现 ${}^4T_1 \rightarrow {}^6A_1$ 的辐射跃迁。在此过程中,Mn作为发光中心的引入,提高了OIMHs的PLQY。

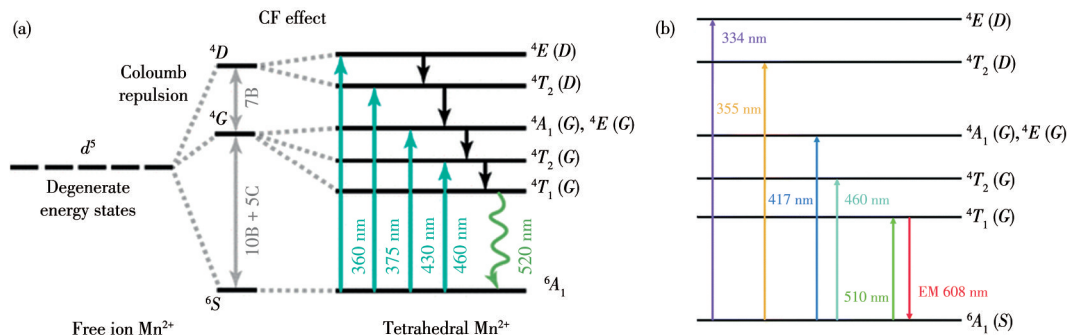


图8 (a) $(\text{Bz}(\text{Me})_3\text{N})_2\text{MnCl}_4$ 在绿光发射下的 $d-d$ 跃迁^[73];(b) $(\text{CH}_3\text{NH}_3)_2\text{MnCl}_4$ 在红光发射下的 $d-d$ 跃迁,图中CF表示晶体场,EM表示发射^[95]

Fig.8 (a) $d-d$ transition of $(\text{Bz}(\text{Me})_3\text{N})_2\text{MnCl}_4$ under green light emission^[73]; (b) $d-d$ transition of $(\text{CH}_3\text{NH}_3)_2\text{MnCl}_4$ under red light emission , where CF represents crystal field and EM represents emission^[95]

2.4 混合机理

对于多中心金属阳离子化合物,其发光中心也

在随之增加,相应的发射机理也会随之改变,通常包含以上几种机理或者引入一些新的机理:(1)有机

发光中心和无机发光中心同时存在。Yue课题组^[27]合成出的化合物[H₂BPP]Pb₂X₆存在2个发射峰,高能峰来自[H₂BPP]²⁺的发射,低能峰来自[Pb₂X₆]²⁻。(2)金属-配体电荷转移或卤化物-配体电荷转移(MLCT/HLCT)、簇中心(CC)相互作用。Xia课题组^[57]

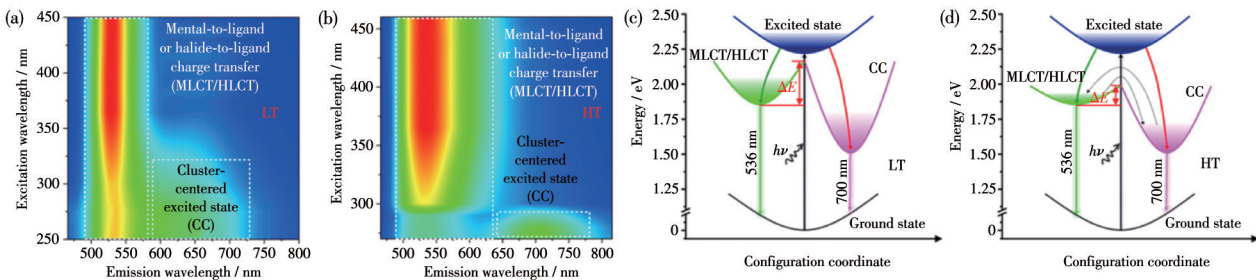


图9 CNCI在(a)低温(LT, 15 K)和(b)高温(HT, 298 K)下的连续PL/PLE相关图;(c) LT和(d) HT的发射机理示意图^[57]

Fig.9 Consecutive PL/PLE correlation charts of CNCI (a) at a low temperature (LT, 15 K) and (b) at a high temperature (HT, 298 K); Schematic diagram of the emission mechanism at (c) LT and (d) HT^[57]

3 提高OIMHs的光致PLQY的方法

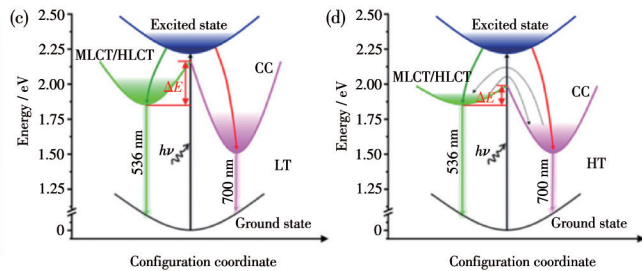
目前提高OIMHs化合物PLQY的策略,主要通过降低晶体结构维度、掺杂发光中心离子、改变配位多面体之间的距离和卤素替代方式对结构进行调节等。

3.1 降低晶体结构维度

降低钙钛矿材料的维度可以调节它们的光学特性^[1]。由于角共享的BX₆八面体晶体结构,使得3D的ABX₃结构具有刚性结构约束,通过增加有机阳离子的长度,可以增加其结构的灵活性,从而实现结构维度的调节。长链烷基铵有机-无机杂化卤化物钙钛矿分子式为A'₂BX₄,通常被称为2D钙钛矿。这里A'是长有机烷基铵阳离子。大多数报道的2D钙钛矿衍生物具有单铵和二铵阳离子,通式为(NH₃RNH₃)BX₄或(RNH₃)₂BX₄,R为有机官能团。对于化合物而言,随着结构维度的降低,化合物的带隙会增加。其中低维材料是天然的量子阱结构,由于量子阱内势垒之间不同的介电环境产生了强烈的电子-空穴相互作用,使得它们具有较大的激子结合能(>100 meV)。这提高了PL强度,并且高量子产率也得益于禁阻电子跃迁的减少^[1]。同时随着维度的降低,STE的束缚能力越来越强,相应会形成一个宽谱发射^[10]。因此,结构灵活、低维金属卤化物的强约束广泛适用于发光应用。

目前报道的PLQY较高的OIMHs主要集中在1D和0D结构中。Ma课题组^[96]报道表明(PEA)₂SnBr₄(2D)的PLQY极低(<0.1%),主要原因就是该化合物

合成出的化合物(18-crown-6)₂Na₂(H₂O)₃Cu₄I₆(CNCl)的光谱图呈现出双发射,其中高能发射峰位于536 nm,低能发射峰位于700 nm,其高能发射峰归因于MLCT/HLCT,低能发射峰归因于CC(图9a~9d, PLE=光致发光激发)。



的非局域化电子态导致较弱的激子结合、较高的激子迁移率和较高的非辐射衰变。在其合成方法中加入了二氯甲烷,形成了[(PEA)₄SnBr₆]][(PEA)Br]₂[CCl₂H₂]₂(OD),其PLQY高达90%,主要就是因为激子的高度局域化,导致了强烈的激子-声子耦合作用。Mao等^[9]合成的(2,6-dmpz)₃Pb₂Br₁₀(1D)是其合成的系列化合物中PLQY最高的,可以达到12%,其发射峰同时具有FE发射和STE发射,此文章中报道的其他2D和3D的化合物都只具有较窄的FE发射。因此,设计、合成具有低维度晶体结构的化合物是实现高PLQY的有效途径之一。本文作者近期研究发现,当OIMHs中有机物为软链结构(不含苯环、双键、三键等刚性结构),同时有机物与无机八面体作用的位点(如N)空间位阻大时,形成的化合物PLQY相对较高^[11,36,81,84,88]。

3.2 掺杂发光中心离子

使用Sb³⁺、Mn²⁺和Sn²⁺等激活剂进行掺杂,可以引入发光中心(图10)。Chen课题组^[97]在InCl₆(C₄H₁₀SN)₄·Cl中掺入Sb³⁺,其PLQY从20%提高到90%,Sb³⁺的引入造成激子的局域化,呈现出宽带发射和大的Stokes位移。对于Sb³⁺掺杂的化合物还有很多^[98-100],比如(C₈NH₁₂)₆InBr₉·H₂O,该化合物PLQY也得到了极大的提升,通过调整浓度实现了白光发射。对于Mn²⁺掺杂^[31,89,101-107]的研究更为普遍,Kundu课题组^[105]报道Mn²⁺掺杂(C₄H₉NH₃)PbBr₄,PLQY最高可达37%,强束缚激子从基质材料到Mn²⁺发生能量转移,从而产生⁴T₁→⁴A₁发射。Gautier课题组^[31]也做

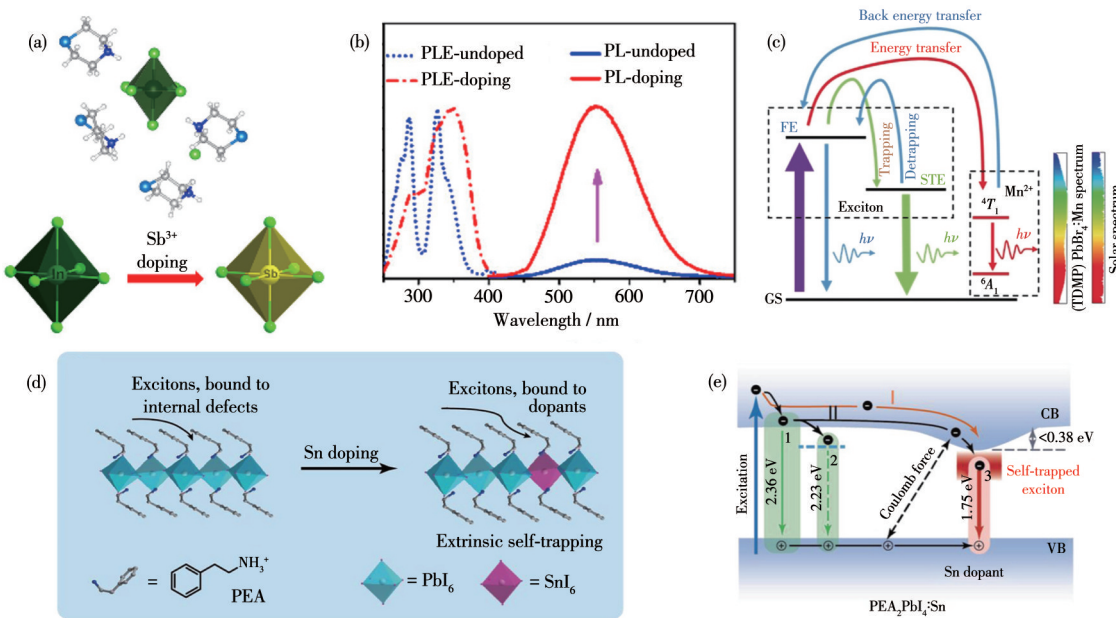


图10 (a) 在 $\text{InCl}_6(\text{C}_4\text{H}_{10}\text{SN})_4 \cdot \text{Cl}$ 中进行 Sb^{3+} 掺杂的替代过程示意图;(b) Sb^{3+} 掺杂和未掺杂 $\text{InCl}_6(\text{C}_4\text{H}_{10}\text{SN})_4 \cdot \text{Cl}$ 的稳态光谱图^[97];(c) $(\text{TDMP})\text{PbBr}_4:\text{Mn}$ 的发光机理^[31];(d) 未掺杂和掺杂Sn的2D钙钛矿晶体中的激子捕获示意图;(e) Sn掺杂 $(\text{PEA})_2\text{PbI}_4$ 辐射通道示意图^[108]

Fig.10 (a) Schematic diagram of the substitution process for Sb^{3+} doping in $\text{InCl}_6(\text{C}_4\text{H}_{10}\text{SN})_4 \cdot \text{Cl}$; (b) Steady-state spectra of Sb^{3+} doped and undoped $\text{InCl}_6(\text{C}_4\text{H}_{10}\text{SN})_4 \cdot \text{Cl}$ ^[97]; (c) Mechanism of luminescence for $(\text{TDMP})\text{PbBr}_4:\text{Mn}$ ^[31]; (d) Schematic illustration of exciton trapping in undoped and Sn-doped 2D perovskite crystals; (e) Schematic illustration of radiative channels in Sn-doped 2D perovskites^[108]

了相关的研究,在($\text{TDMP})\text{PbBr}_4$ 中掺入 Mn^{2+} ,其PLQY可以达到60%。关于 Sn^{2+} 掺杂的研究较少,Chen课题组^[108]在($\text{PEA})_2\text{PbI}_4$ 中掺入 Sn^{2+} ,实现了PLQY从0.7%到6%增加。对OIMHs材料进行掺杂,实现高效、宽带发光,已经成为了当前提高该类材料荧光性能的主要途径之一。

3.3 改变配位多面体之间的距离

通过选择有机阳离子增加 Mn-Mn 之间的距

离^[72,109-110],减少能量转移,可实现高效发光(图11a、11b)。也有研究表明,并不是距离越远越好, $\text{Mn}-\text{Mn}$ 距离增加到0.925 4 nm,其PLQY达到最大,之后随距离增加其PLQY反而开始降低^[111]。

3.4 卤素替代

对于杂化金属卤化物发光材料而言,其发光主要来自无机结构 $[\text{BX}_6]^{2-}$ 、 $[\text{BX}_4]^{2-}$ 等,随着B位置上金属离子不同,PLQY会发生改变;同样其配位卤素发

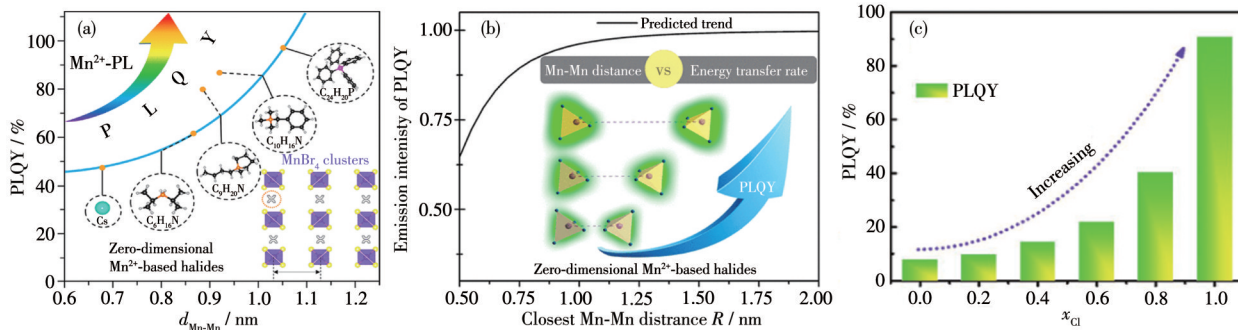


图11 (a) 所选的OD Mn^{2+} 基金属卤化物的最近 $\text{Mn}-\text{Mn}$ 距离和PLQY的图示;(b) 预测OD Mn^{2+} 基金属卤化物中 Mn^{2+} 的发射强度与最近 $\text{Mn}-\text{Mn}$ 距离的依赖关系^[109];(c) Cl 元素含量与PLQY变化之间的关系^[112]

Fig.11 (a) Illustration of the closest Mn-Mn distance and PLQY for the selected 0D Mn^{2+} -based metal halides; (b) Predicted dependences of the emission intensity of Mn^{2+} on the closest Mn-Mn distance in 0D Mn^{2+} -based metal halides^[109]; (c) Relationship between the content of Cl element and the change of PLQY^[112]

生改变,也会严重地影响发光基团,从而影响PLQY^[10]。如图11c所示,Xia课题组^[112]报道随着 $(\text{C}_9\text{NH}_{20})_9\text{Pb}_3\text{Zn}_2\text{Br}_{19(1-x)}\text{Cl}$ ($x=0\sim 1$)中 x 的增加其发射峰位不断蓝移,同时PLQY从8%增加到91%。其中随着Cl含量的增加,热辅助非辐射复合作用减弱,产生更有效的辐射跃迁通道,最终使PLQY增强。

4 稳定性

对于OIMHs而言,其稳定性是制约发展的关键,目前并未形成可以提高其稳定性的统一理论。针对A位而言,引入大的含硫有机阳离子与中心金属阳离子进行有机构筑,其中阳离子半径需要大于Cs、MA和FA,其形成的化合物更倾向生成低维度结构,结构维度的降低可以提高化合物的稳定性。对于金属离子而言,目前稳定性较高的是 Sn^{4+} ,此前Lin课题组^[53]合成出的 $(\text{C}_6\text{N}_2\text{H}_{16}\text{Cl})_2\text{SnCl}_6$ 在高达523 K(250 °C)的温度下表现出显著的空气和热稳定性。He课题组^[113]合成的 $(\text{C}_8\text{H}_{22}\text{Cl})_2\text{SnCl}_6$ 在高温(>200 °C)和高湿度(相对湿度大于70%)下均表现出显著的结构稳定性。其他金属离子也用于合成有高稳定性的化合物,如 $(\text{TMA})_2\text{SbCl}_5 \cdot \text{DMF}$ ^[114]、 $[\text{H}_2\text{DABCO}] [\text{Ag}_2\text{Br}_4(\text{DABCO})]$ ^[64]、MEA(MnBr_4)₂(MEA = $((\text{CH}_3)_4\text{N})((\text{C}_2\text{H}_5)_4\text{N})_2 \cdot \text{NH}_4$)^[115]、 $(\text{C}_{24}\text{H}_{20}\text{P})_2\text{MnBr}_4$ ^[71]等。

5 总结与展望

本文主要总结了高效的OIMHs,按照B位金属阳离子的不同电子特征进行分类(ns^2 、 d^{10} 、 d^5),当前研究显示仍然是 ns^2 系列OIMHs的PLQY最高, Pb^{2+} 的毒性制约了其进一步发展, Sn^{2+} 基材料中高效发光的较多,但是其室温稳定性问题阻碍了其应用的步伐。 d^{10} 系列金属阳离子最为丰富,每种金属阳离子都有不同的特性,丰富了OIMHs的光学性能。 d^5 系列的 Mn^{2+} 可以形成立体发光中心,正在成为单中心金属阳离子、多中心金属阳离子以及掺杂OIMHs争相研究的重点。不同类型的发光材料,其发光机理不尽相同,目前比较认可的机理主要包括:STE发光、 ns^2 孤对电子发光、 Mn^{2+} 的孤立发光中心以及混合发光机理。其中在低维的金属卤化物研究中,仍以STE发光为主。 d^{10} 系列化合物中的宽带发射机理尚不清楚,当前主要使用STE模型进行解释。为了制备出更加高效的发光材料,通常会尝试使用降低结构维度、掺杂、调整发光中心之间的距离以及卤素共取代等措施,产生宽带发射同时提高PLQY。

这些材料的持续开发将推动OIMHs发光材料领域新一轮的研究热潮并最终促进其商业应用。

然而,合成高效的OIMHs发光材料的未来发展仍然面临许多挑战,包括但不限于:

(1) 热稳定性。虽然目前已经合成了高效率的发光材料,但是随着温度的升高,其PLQY就会骤降(热猝灭)。提高其在70 °C左右(商业LED表面温度)的热猝灭性能是实现其商业化的关键一步。

(2) 有机物对PLQY的影响尚不清楚。即使是相同的金属阳离子,当有机阳离子不同时,其PLQY也不尽相同。

(3) 实现单一组分白光发射仍然存在困难,目前通过调整多中心金属阳离子可以实现白光发射,但是其PLQY比较低。

(4) 对于 d^{10} 系列的金属阳离子研究还较少,其发光机理仍不清楚,此方面还需要更多的理论研究。

参考文献:

- [1]Quan L N, Rand B P, Friend R H, Mhaisalkar S G, Lee T W, Sargent E H. Perovskites for Next-Generation Optical Sources. *Chem. Rev.*, **2019**, *119*(12):7444-7477
- [2]Liu X K, Xu W, Bai S, Jin Y, Wang J, Friend R H, Gao F. Metal Halide Perovskites for Light-Emitting Diodes. *Nat. Mater.*, **2021**, *20*(1):10-21
- [3]Yao J S, Wang J J, Yang J N, Yao H B. Modulation of Metal Halide Structural Units for Light Emission. *Acc. Chem. Res.*, **2021**, *54*(2):441-451
- [4]苑帅, 沈万姗, 廖良生. 基于金属卤化物钙钛矿材料的高效发光二极管. *物理*, **2021**, *50*(6):385-392
YUAN S, SHEN W S, LIAO L S. High-Efficiency Light-Emitting Diode Based on Metal Halide Perovskite Material. *Physics*, **2021**, *50*(6):385-392
- [5]Philippe B, Jacobsson T J, Correa-Baena J P, Jena N K, Banerjee A, Chakraborty S, Cappel U B, Ahuja R, Hagfeldt A, Odelius M, Rensmo H. Valence Level Character in a Mixed Perovskite Material and Determination of the Valence Band Maximum from Photoelectron Spectroscopy: Variation with Photon Energy. *J. Phys. Chem. C*, **2017**, *121*(48):26655-26666
- [6]Liu H W, Wu Z N, Gao H, Shao J R, Zou H Y, Yao D, Liu Y, Zhang H, Yang B. One-Step Preparation of Cesium Lead Halide CsPbX_3 ($X=\text{Cl}, \text{Br}$, and I) Perovskite Nanocrystals by Microwave Irradiation. *ACS Appl. Mater. Interfaces*, **2017**, *9*(49):42919-42927
- [7]Zhang F, Zhong H Z, Chen C, Wu X G, Hu X M, Huang H L, Han J B, Zou B S, Dong Y P. Brightly Luminescent and Color-Tunable Colloidal $\text{CH}_3\text{NH}_3\text{PbX}_3$ ($X=\text{Br}, \text{I}, \text{Cl}$) Quantum Dots: Potential Alterna-

- tives for Display Technology. *ACS Nano*, **2015**,*9*(4):4533-4542
- [8]Li M Z, Xia Z G. Recent Progress of Zero-Dimensional Luminescent Metal Halides. *Chem. Soc. Rev.*, **2021**,*50*(4):2626-2662
- [9]Mao L L, Guo P J, Kepenekian M, Hadar I, Katan C, Even J, Schaller R D, Stoumpos C C, Kanatzidis M G. Structural Diversity in White-Light-Emitting Hybrid Lead Bromide Perovskites. *J. Am. Chem. Soc.*, **2018**,*140*(40):13078-13088
- [10]McCall K M, Morad V, Benin B M, Kovalenko M V. Efficient Lone-Pair - Driven Luminescence: Structure - Property Relationships in Emissive $5s^2$ Metal Halides. *ACS Mater. Lett.*, **2020**,*2*(9):1218-1232
- [11]Yuan Z, Zhou C K, Tian Y, Shu Y, Messier J, Wang J C, van de Burgt L J, Kountouriotis K, Xin Y, Holt E, Schanze K, Clark R, Siegrist T, Ma B W. One-Dimensional Organic Lead Halide Perovskites with Efficient Bluish White-Light Emission. *Nat. Commun.*, **2017**,*8*:14051
- [12]Qi Z K, Chen Y L, Guo Y, Yang X L, Gao H Z, Zhou G J, Li S L, Zhang X M. Highly Efficient Self-Trapped Exciton Emission in a One-Dimensional Face-Shared Hybrid Lead Bromide. *Chem. Commun.*, **2021**,*57*(20):2495-2498
- [13]Deng C K, Hao S Q, Liu K J, Molokeev M S, Wolverton C, Fan L B, Zhou G J, Chen D, Zhao J, Liu Q L. Broadband Light Emitting Zero-Dimensional Antimony and Bismuth - Based Hybrid Halides with Diverse Structures. *J. Mater. Chem. C*, **2021**,*9*(44):15942-15948
- [14]Chen D, Hao S Q, Fan L B, Guo Y W, Yao J Y, Wolverton C, Kanatzidis M G, Zhao J, Liu Q L. Broad Photoluminescence and Second-Harmonic Generation in the Noncentrosymmetric Organic-Inorganic Hybrid Halide $(C_6H_5(CH_2)_4NH_3)_4MX_7 \cdot H_2O$ ($M=Bi$, In, X=Br or I). *Chem. Mater.*, **2021**,*33*:8106-8111
- [15]Chen D, Dai F L, Hao S Q, Zhou G J, Liu Q L, Wolverton C, Zhao J, Xia Z G. Crystal Structure and Luminescence Properties of Lead-Free Metal Halides $(C_6H_5CH_2NH_3)_3MBr_6$ ($M=Bi$ and Sb). *J. Mater. Chem. C*, **2020**,*8*(22):7322-7329
- [16]Liu K J, Deng C K, Li C X, Zhang X S, Cao J D, Yao J Y, Zhao J, Jiang X X, Lin Z S, Liu Q L. Hybrid Metal-Halide Infrared Nonlinear Optical Crystals of $(TMEDA)M_3$ ($M=Sb$, Bi) with High Stability. *Adv. Opt. Mater.*, **2021**,*9*(24):2101333
- [17]Hao P F, Wang W P, Shen J J, Fu Y L. Non-Transient Thermo-/Photochromism of Iodobismuthate Hybrids Directed by Solvated Met-al Cations. *Dalton Trans.*, **2020**,*49*(6):1847-1853
- [18]Dehnhardt N, Paneth H, Hecht N, Heine J. Multinary Halogenido Bismuthates beyond the Double Perovskite Motif. *Inorg. Chem.*, **2020**,*59*(6):3394-3405
- [19]Dohner E R, Jaffe A, Bradshaw L R, Karunadasa H I. Intrinsic White-Light Emission from Layered Hybrid Perovskites. *J. Am. Chem. Soc.*, **2014**,*136*(38):13154-13157
- [20]Morad V, Shynkarenko Y, Yakunin S, Brumberg A, Schaller R D, Kovalenko M V. Disphenoidal Zero-Dimensional Lead, Tin, and Germanium Halides: Highly Emissive Singlet and Triplet Self-Trapped Excitons and X-ray Scintillation. *J. Am. Chem. Soc.*, **2019**,*141*(25):9764-9768
- [21]Gong L K, Huang F Q, Zhang Z Z, Zhong Y, Jin J C, Du K Z, Huang X Y. Multimode Dynamic Luminescent Switching of Lead Halide Hybrids for Anti - counterfeiting and Encryption. *Chem. Eng. J.*, **2021**,*424*:130544
- [22]Lin H R, Zhou C K, Chaaban M, Xu L J, Zhou Y, Neu J, Worku M, Berkwits E, He Q Q, Lee S J, Lin X S, Siegrist T, Du M H, Ma B W. Bulk Assembly of Zero-Dimensional Organic Lead Bromide Hybrid with Efficient Blue Emission. *ACS Mater. Lett.*, **2019**,*1*(6):594-598
- [23]Dhanabalan B, Castelli A, Palei M, Spirito D, Manna L, Krahne R, Arciniegas M. Simple Fabrication of Layered Halide Perovskite Platelets and Enhanced Photoluminescence from Mechanically Exfoliated Flakes. *Nanoscale*, **2019**,*11*(17):8334-8342
- [24]Dou L T, Wong A B, Yu Y, Lai M L, Kornienko N, Eaton S W, Fu A, Bischak C G, Ma J, Ding T, Ginsberg N S, Wang L W, Alivisatos A P, Yang P. Atomically Thin Two - Dimensional Organic - Inorganic Hybrid Perovskites. *Science*, **2015**,*349*(6255):1518-1521
- [25]Cui B B, Han Y, Huang B L, Zhao Y Z, Wu X X, Liu L, Cao G Y, Du Q, Liu N, Zou W, Sun M Z, Wang L, Liu X F, Wang J P, Zhou H P, Chen Q. Locally Collective Hydrogen Bonding Isolates Lead Octahedra for White Emission Improvement. *Nat. Commun.*, **2019**,*10*(1):5190
- [26]Lin H R, Zhou C K, Neu J, Zhou Y, Han D, Chen S Y, Worku M, Chaaban M, Lee S J, Berkwits E, Siegrist T, Du M H, Ma B W. Bulk Assembly of Corrugated 1D Metal Halides with Broadband Yellow Emission. *Adv. Opt. Mater.*, **2019**,*7*(6):1801474
- [27]Sun X Y, Yue M, Jiang Y X, Zhao C H, Liao Y Y, Lei X W, Yue C Y. Combining Dual-Light Emissions to Achieve Efficient Broadband Yellowish-Green Luminescence in One-Dimensional Hybrid Lead Halides. *Inorg. Chem.*, **2021**,*60*(3):1491-1498
- [28]Zhang W F, Pan W J, Xu T, Song R Y, Zhao Y Y, Yue C Y, Lei X W. One-Dimensional Face-Shared Perovskites with Broad-Band Bluish White-Light Emissions. *Inorg. Chem.*, **2020**,*59*(19):14085-14092
- [29]Yang W T, Xiao X L, Li M K, Hu J R, Xiao X F, Tong G L, Chen J N, He Y B. Conjugated Diteriary Ammonium Tempered (100)-Oriented 2D Perovskite with Efficient Broad-Band Emission. *Chem. Mater.*, **2021**,*33*(12):4456-4464
- [30]Wu S Q, Zhou B, Yan D P. Low-Dimensional Organic Metal Halide Hybrids with Excitation-Dependent Optical Waveguides from Visible to Near-Infrared Emission. *ACS Appl. Mater. Interfaces*, **2021**,*13*(22):26451-26460
- [31]Yuan H L, Massuyeau F, Gautier N, Kama A B, Faulques E, Chen F, Shen Q, Zhang L M, Paris M, Gautier R. Doped Lead Halide White Phosphors for Very High Efficiency and Ultra-High Color Rendering. *Angew. Chem. Int. Ed.*, **2020**,*59*(7):2802-2807
- [32]Zhou J, Li M Z, Ning L X, Zhang R L, Molokeev M S, Zhao J, Yang S Q, Han K L, Xia Z G. Broad-Band Emission in a Zero-Dimensional Hybrid Organic $[PbBr_6]$ Trimer with Intrinsic Vacancies. *J. Phys. Chem. Lett.*, **2019**,*10*(6):1337-1341
- [33]Shi H L, Han D, Chen S Y, Du M H. Impact of Metal ns^2 Lone Pair on Luminescence Quantum Efficiency in Low-Dimensional Halide Perovskites. *Phys. Rev. Mater.*, **2019**,*3*(3):034604
- [34]Fu Y P, Jin S, Zhu X Y. Stereochemical Expression of ns^2 Electron

- Pairs in Metal Halide Perovskites. *Nat. Rev. Chem.*, **2021**, *5*(12):838-852
- [35] Liu X Y, Li Y Y, Liang T Y, Fan J Y. Role of Polyhedron Unit in Distinct Photophysics of Zero-Dimensional Organic-Inorganic Hybrid Tin Halide Compounds. *J. Phys. Chem. Lett.*, **2021**, *12*(24):5765-5773
- [36] Zhou C K, Lin H R, Tian Y, Yuan Z, Clark R, Chen B H, Van De Burgt L J, Wang J C, Zhou Y, Hanson K, Meisner Q J, Neu J, Besara T, Siegrist T, Lambers E, Djurovich P, Ma B W. Luminescent Zero-Dimensional Organic Metal Halide Hybrids with Near-Unity Quantum Efficiency. *Chem. Sci.*, **2018**, *9*(3):586-593
- [37] Biswas A, Bakthavatsalam R, Bahadur V, Biswas C, Mali B P, Raavi S S K, Gonnade R G, Kundu J. Lead-Free Zero Dimensional Tellurium(IV) Chloride-Organic Hybrid with Strong Room Temperature Emission as a Luminescent Material. *J. Mater. Chem. C*, **2021**, *9*(12):4351-4358
- [38] Wang A F, Guo Y Y, Zhou Z B, Niu X H, Wang Y G, Muhammad F, Li H B, Zhang T, Wang J L, Nie S M, Deng Z T. Aqueous Acid-Based Synthesis of Lead-Free Tin Halide Perovskites with Near-Unity Photoluminescence Quantum Efficiency. *Chem. Sci.*, **2019**, *10*(17):4573-4579
- [39] Fu P F, Huang M L, Shang Y Q, Yu N, Zhou H L, Zhang Y B, Chen S Y, Gong J K, Ning Z J. Organic-Inorganic Layered and Hollow Tin Bromide Perovskite with Tunable Broadband Emission. *ACS Appl. Mater. Interfaces*, **2018**, *10*(40):34363-34369
- [40] Wang S X, Popović J, Burazer S, Portniagin A, Liu F Z, Low K H, Duan Z H, Li Y X, Xiong Y, Zhu Y M, Kershaw S V, Djurišić A B, Rogach A L. Strongly Luminescent Dion-Jacobson Tin Bromide Perovskite Microcrystals Induced by Molecular Proton Donors Chloroform and Dichloromethane. *Adv. Funct. Mater.*, **2021**, *31*(28):2102182
- [41] Su B B, Song G M, Molokeev M S, Lin Z S, Xia Z G. Synthesis, Crystal Structure and Green Luminescence in Zero-Dimensional Tin Halide ($C_8H_{14}N_2$)₂SnBr₆. *Inorg. Chem.*, **2020**, *59*(14):9962-9968
- [42] Wolf S, Liebertseder M, Feldmann C. Synthesis, Structure, and Photoluminescence of the Chloridoaluminates [BMIm][Sn(AlCl₄)₃], [BMPy][Sn(AlCl₄)₃], and [BMIm][Pb(AlCl₄)₃]. *Dalton Trans.*, **2021**, *50*(24):8549-8557
- [43] Zhou C K, Worku M, Neu J, Lin H R, Tian Y, Lee S J, Zhou Y, Han D, Chen S Y, Hao A, Djurovich P I, Siegrist T, Du M H, Ma B W. Facile Preparation of Light Emitting Organic Metal Halide Crystals with Near-Unity Quantum Efficiency. *Chem. Mater.*, **2018**, *30*(7):2374-2378
- [44] Li Z Y, Li Y, Liang P, Zhou T L, Wang L, Xie R J. Dual-Band Luminescent Lead-Free Antimony Chloride Halides with Near-Unity Photoluminescence Quantum Efficiency. *Chem. Mater.*, **2019**, *31*(22):9363-9371
- [45] Morad V, Yakunin S, Benin B M, Shynkarenko Y, Grotevent M J, Shorubalko I, Boehme S C, Kovalenko M V. Hybrid 0D Antimony Halides as Air-Stable Luminophores for High-Spatial-Resolution Remote Thermography. *Adv. Mater.*, **2021**, *33*(9):e2007355
- [46] He Q Q, Zhou C K, Xu L J, Lee S J, Lin X S, Neu J, Worku M, Chaaban M, Ma B W. Highly Stable Organic Antimony Halide Crystals for X-ray Scintillation. *ACS Mater. Lett.*, **2020**, *2*(6):633-638
- [47] Chen D, Hao S Q, Zhou G J, Deng C K, Liu Q L, Ma S L, Wolverton C, Zhao J, Xia Z G. Lead-Free Broadband Orange-Emitting Zero-Dimensional Hybrid (PMA)₃InBr₆ with Direct Band Gap. *Inorg. Chem.*, **2019**, *58*(22):15602-15609
- [48] Fattal H, Creason T D, Delzer C J, Yangui A, Hayward J P, Ross B J, Du M H, Glatzhofer D T, Saparov B. Zero-Dimensional Hybrid Organic-Inorganic Indium Bromide with Blue Emission. *Inorg. Chem.*, **2021**, *60*(2):1045-1054
- [49] 王申宇, 陈典, 刘晓莉, 王硕文, 苑亚南, 王振平, 杨春. 基于(*E*-*N*,*N*-二甲基-4-(2-(吡啶-4-基)乙烯基)苯胺的锌/镉有机-无机杂化金属卤化物的结构和发光性质. *无机化学学报*, **2021**, *37*(9):1659-1664
- WANG S Y, CHEN D, LIU X L, WANG S W, YUAN Y N, WANG Z P, YANG C. Structures and Photoluminescence Properties of Zinc(II)/Cadmium (II)-Based Organic-Inorganic Hybrid Metal Halides Derived from (*E*-*N,N*-Dimethyl-4-(2-(pyridin-4-yl)vinyl) aniline. *Chinese J. Inorg. Chem.*, **2021**, *37*(9):1659-1664
- [50] Xu L J, Plaviak A, Lin X S, Worku M, He Q Q, Chaaban M, Kim B J, Ma B W. Metal Halide Regulated Photophysical Tuning of Zero-Dimensional Organic Metal Halide Hybrids: From Efficient Phosphorescence to Ultralong Afterglow. *Angew. Chem. Int. Ed.*, **2020**, *59*(51):23067-23071
- [51] Lian L Y, Zhang P, Liang G J, Wang S, Wang X, Wang Y, Zhang X W, Gao J B, Zhang D L, Gao L, Song H S, Chen R, Lan X Z, Liang W X, Niu G D, Tang J, Zhang J B. Efficient Dual-Band White-Light Emission with High Color Rendering from Zero-Dimensional Organic Copper Iodide. *ACS Appl. Mater. Interfaces*, **2021**, *13*(19):22749-22756
- [52] Zhang R C, Wang J J, Zhang J C, Wang M Q, Sun M, Ding F, Zhang D J, An Y L. Coordination-Induced Syntheses of Two Hybrid Framework Iodides: A Thermochromic Luminescent Thermometer. *Inorg. Chem.*, **2016**, *55*(15):7556-7563
- [53] Song G M, Li M Z, Yang Y, Liang F, Huang Q, Liu X M, Gong P F, Xia Z G, Lin Z S. Lead-Free Tin(IV)-Based Organic-Inorganic Metal Halide Hybrids with Excellent Stability and Blue-Broadband Emission. *J. Phys. Chem. Lett.*, **2020**, *11*(5):1808-1813
- [54] Peng H, Tian Y, Zhang Z H, Wang X X, Huang T, Dong T T, Xiao Y H, Wang J P, Zou B S. Bulk Assembly of Zero-Dimensional Organic Copper Bromide Hybrid with Bright Self-Trapped Exciton Emission and High Antiwater Stability. *J. Phys. Chem. C*, **2021**, *125*(36):20014-20021
- [55] Liu F, Mondal D, Zhang K, Zhang Y, Huang K K, Wang D Y, Yang W S, Mahadevan P, Xie R G. Zero-Dimensional Plate-Shaped Copper Halide Crystals with Green-Yellow Emissions. *Mater. Adv.*, **2021**, *2*(11):3744-3751
- [56] Peng H, Wang X X, Tian Y, Zou B S, Yang F, Huang T, Peng C Y, Yao S F, Yu Z M, Yao Q R, Rao G H, Wang J Q. Highly Efficient Cool-White Photoluminescence of (Gua)₃Cu₂I₅ Single Crystals: Formation and Optical Properties. *ACS Appl. Mater. Interfaces*, **2021**, *13*

- (11):13443-13451
- [57]Huang J L, Su B B, Song E H, Molokeev M S, Xia Z G. Ultra-Broad-Band-Excitable Cu(I)-Based Organometallic Halide with Near-Unity Emission for Light-Emitting Diode Applications. *Chem. Mater.*, **2021**,*33*(12):4382-4389
- [58]Wang S X, Morgan E E, Vishnoi P, Mao L L, Teicher S M L, Wu G, Liu Q L, Cheetham A K, Seshadri R. Tunable Luminescence in Hybrid Cu(I) and Ag(I) Iodides. *Inorg. Chem.*, **2020**,*59*(20):15487-15494
- [59]Huitorel B, El Moll H, Utrera-Melero R, Cordier M, Fargues A, Garcia A, Massuyeau F, Martineau-Corcos C, Fayon F, Rakhmatullin A, Kahlal S, Saillard J Y, Gacoin T, Perruchas S. Evaluation of Ligands Effect on the Photophysical Properties of Copper Iodide Clusters. *Inorg. Chem.*, **2018**,*57*(8):4328-4339
- [60]Utrera-Melero R, Huitorel B, Cordier M, Mevellec J Y, Massuyeau F, Latouche C, Martineau-Corcos C, Perruchas S. Combining Theory and Experiment to Get Insight into the Amorphous Phase of Luminescent Mechanochromic Copper Iodide Clusters. *Inorg. Chem.*, **2020**,*59*(18):13607-13620
- [61]Perruchas S, Tard C, Le Goff X F, Fargues A, Garcia A, Kahlal S, Saillard J Y, Gacoin T, Boilot J P. Thermochromic Luminescence of Copper Iodide Clusters: The Case of Phosphine Ligands. *Inorg. Chem.*, **2011**,*50*(21):10682-10692
- [62]Yangui A, Rocanova R, McWhorter T M, Wu Y T, Du M H, Saparov B. Hybrid Organic-Inorganic Halides ($C_5H_7N_2$)₂MBr₄ (M=Hg, Zn) with High Color Rendering Index and High-Efficiency White-Light Emission. *Chem. Mater.*, **2019**,*31*(8):2983-2991
- [63]Zhang X Y, Li L, Wang S S, Liu X T, Yao Y P, Peng Y, Hong M C, Luo J H. [(N-AEPz)ZnCl₄]Cl: A “Green” Metal Halide Showing Highly Efficient Bluish-White-Light Emission. *Inorg. Chem.*, **2020**,*59*(6):3527-3531
- [64]Sun C, Guo Y H, Yuan Y, Chu W X, He W L, Che H X, Jing Z H, Yue C Y, Lei X W. Broadband White-Light Emission in One-Dimensional Organic-Inorganic Hybrid Silver Halide. *Inorg. Chem.*, **2020**,*59*(7):4311-4319
- [65]Gong L K, Hu Q Q, Huang F Q, Zhang Z Z, Shen N N, Hu B, Song Y, Wang Z P, Du K Z, Huang X Y. Efficient Modulation of Photoluminescence by Hydrogen Bonding Interactions between Inorganic [MnBr₄]²⁻ Anions and Organic Cations. *Chem. Commun.*, **2019**,*55*(51):7303-7306
- [66]Wang S Y, Han X X, Kou T T, Zhou Y Y, Liang Y, Wu Z X, Huang J L, Chang T, Peng C Y, Wei Q L, Zou B S. Lead-Free Mn^{II}-Based Red-Emitting Hybrid Halide (CH₆N₃)₂MnCl₄ toward High Performance Warm WLEDs. *J. Mater. Chem. C*, **2021**,*9*(14):4895-4902
- [67]Jana A, Zhumagali S, Ba Q K, Nissimogoudar A S, Kim K S. Direct Emission from Quartet Excited States Triggered by Upconversion Phenomena in Solid-Phase Synthesized Fluorescent Lead-Free Organic-Inorganic Hybrid Compounds. *J. Mater. Chem. A*, **2019**,*7*(46):26504-26512
- [68]Li M Z, Zhou J, Molokeev M S, Jiang X X, Lin Z S, Zhao J, Xia Z G. Lead-Free Hybrid Metal Halides with a Green-Emissive [MnBr₄] Unit as a Selective Turn-On Fluorescent Sensor for Acetone. *Inorg. Chem.*, **2019**,*58*(19):13464-13470
- [69]Li L Y, Li L, Li Q Q, Shen Y M, Pan S K, Pan J G. Synthesis, Crystal Structure and Optical Property of Manganese(II) Halides Based on Pyridine Ionic Liquids with High Quantum Yield. *Transition. Met. Chem.*, **2020**,*45*(6):413-421
- [70]Zhang S, Zhao Y F, Zhou Y Y, Li M, Wang W, Ming H, Jing X P, Ye S. Dipole-Orientation-Dependent Förster Resonance Energy Transfer from Aromatic Head Groups to MnBr₄²⁻ Blocks in Organic-Inorganic Hybrids. *J. Phys. Chem. Lett.*, **2021**,*12*(36):8692-8698
- [71]Zhou G J, Liu Z Y, Molokeev M S, Xiao Z W, Xia Z G, Zhang X M. Manipulation of Cl/Br Transmutation in Zero-Dimensional Mn²⁺-Based Metal Halides toward Tunable Photoluminescence and Thermal Quenching Behaviors. *J. Mater. Chem. C*, **2021**,*9*(6):2047-2053
- [72]Mao L L, Guo P J, Wang S X, Cheetham A K, Seshadri R. Design Principles for Enhancing Photoluminescence Quantum Yield in Hybrid Manganese Bromides. *J. Am. Chem. Soc.*, **2020**,*142*(31):13582-13589
- [73]Morad V, Cherninkh I, Pottschacher L, Shynkarenko Y, Yakunin S, Kovalenko M V. Manganese(II) in Tetrahedral Halide Environment: Factors Governing Bright Green Luminescence. *Chem. Mater.*, **2019**,*31*(24):10161-10169
- [74]Zhao J, Zhang T J, Dong X Y, Sun M E, Zhang C, Li X L, Zhao Y S, Zang S Q. Circularly Polarized Luminescence from Achiral Single Crystals of Hybrid Manganese Halides. *J. Am. Chem. Soc.*, **2019**,*141*(40):15755-15760
- [75]Sun M E, Li Y, Dong X Y, Zang S Q. Thermoinduced Structural-Transformation and Thermochromic Luminescence in Organic Manganese Chloride Crystals. *Chem. Sci.*, **2019**,*10*(13):3836-3839
- [76]Jiang X M, Chen Z L, Tao X T. (1-C₅H₁₄N₂Br)₂MnBr₄: A Lead-Free Zero-Dimensional Organic-Metal Halide with Intense Green Photoluminescence. *Front. Chem.*, **2020**,*8*:352
- [77]Jiang X M, Xia S Q, Zhang J, Ju D X, Liu Y, Hu X B, Wang L, Chen Z L, Tao X T. Exploring Organic Metal Halides with Reversible Temperature-Responsive Dual-Emissive Photoluminescence. *ChemSusChem*, **2019**,*12*(24):5228-5232
- [78]Zhang Y, Liao W Q, Fu D W, Ye H Y, Chen Z N, Xiong R G. Highly Efficient Red-Light Emission in an Organic-Inorganic Hybrid Ferroelectric: (Pyrrolidinium)MnCl₃. *J. Am. Chem. Soc.*, **2015**,*137*(15):4928-4931
- [79]Ye H Y, Zhou Q, Niu X, Liao W Q, Fu D W, Zhang Y, You Y M, Wang J, Chen Z N, Xiong R G. High-Temperature Ferroelectricity and Photoluminescence in a Hybrid Organic-Inorganic Compound: (3-Pyrrolinium)MnCl₃. *J. Am. Chem. Soc.*, **2015**,*137*(40):13148-13154
- [80]Xu L J, Lee S J, Lin X S, Ledbetter L, Worku M, Lin H R, Zhou C K, Liu H, Plaviak A, Ma B W. Multicomponent Organic Metal Halide Hybrid with White Emissions. *Angew. Chem. Int. Ed.*, **2020**,*59*(33):14120-14123
- [81]Li M Z, Molokeev M S, Zhao J, Xia Z G. Optical Functional Units in Zero-Dimensional Metal Halides as a Paradigm of Tunable Photolu-

- minescence and Multicomponent Chromophores. *Adv. Opt. Mater.*, **2020**, *8*(8):1902114
- [82] Zhou C K, Lee S J, Lin H R, Neu J, Chaaban M, Xu L J, Arcidiacono A, He Q Q, Worku M, Ledbetter L, Lin X S, Schlueter J A, Siegrist T, Ma B W. Bulk Assembly of Multicomponent Zero-Dimensional Metal Halides with Dual Emission. *ACS Mater. Lett.*, **2020**, *2*(4):376-380
- [83] Lee S J, Zhou C K, Neu J, Beery D, Arcidiacono A, Chaaban M, Lin H R, Gaiser A, Chen B H, Albrecht-Schmitt T E, Siegrist T, Ma B W. Bulk Assemblies of Lead Bromide Trimer Clusters with Geometry-Dependent Photophysical Properties. *Chem. Mater.*, **2020**, *32*(1):374-380
- [84] Zhou C K, Lin H R, Neu J, Zhou Y, Chaaban M, Lee S J, Worku M, Chen B H, Clark R, Cheng W H, Guan J J, Djurovich P, Zhang D Z, Lü X J, Bullock J, Pak C, Shatruk M, Du M H, Siegrist T, Ma B W. Green Emitting Single-Crystalline Bulk Assembly of Metal Halide Clusters with Near-Unity Photoluminescence Quantum Efficiency. *ACS Energy Lett.*, **2019**, *4*(7):1579-1583
- [85] Li M Z, Zhou J, Zhou G J, Molokeev M S, Zhao J, Morad V, Kovalenko M V, Xia Z G. Hybrid Metal Halides with Multiple Photoluminescence Centers. *Angew. Chem. Int. Ed.*, **2019**, *58*(51):18670-18675
- [86] Zhou C K, Lin H R, Worku M, Neu J, Zhou Y, Tian Y, Lee S J, Djurovich P, Siegrist T, Ma B W. Blue Emitting Single Crystalline Assembly of Metal Halide Clusters. *J. Am. Chem. Soc.*, **2018**, *140*(41):13181-13184
- [87] Zhang Z Z, Jin J C, Gong L K, Lin Y P, Du K Z, Huang X Y. Co-luminescence in a Zero-Dimensional Organic-Inorganic Hybrid Antimony Halide with Multiple Coordination Units. *Dalton Trans.*, **2021**, *50*(10):3586-3592
- [88] Fan L B, Liu K J, Zeng Q D, Li M Y, Cai H, Zhou J, He S H, Zhao J, Liu Q L. Efficiency-Tunable Single-Component White-Light Emission Realized in Hybrid Halides through Metal Co-Occupation. *ACS Appl. Mater. Interfaces*, **2021**, *13*(25):29835-29842
- [89] Peng Y, Li L N, Ji C M, Wu Z Y, Wang S S, Liu X T, Yao Y P, Luo J H. Tailored Synthesis of an Unprecedented Pb-Mn Heterometallic Halide Hybrid with Enhanced Emission. *J. Am. Chem. Soc.*, **2019**, *141*(31):12197-12201
- [90] Smith M D, Karunadasa H I. White-Light Emission from Layered Halide Perovskites. *Acc. Chem. Res.*, **2018**, *51*(3):619-627
- [91] Zhao J Q, Sun C, Yue M, Meng Y, Zhao X M, Zeng L R, Chen G, Yue C Y, Lei X W. Lead Chlorine Cluster Assembled One-Dimensional Halide with Highly Efficient Broadband White-Light Emission. *Chem. Commun.*, **2021**, *57*(10):1218-1221
- [92] Yang B, Chen J S, Hong F, Mao X, Zheng K B, Yang S Q, Li Y J, Pullerits T, Deng W Q, Han K L. Lead-Free, Air-Stable All-Inorganic Cesium Bismuth Halide Perovskite Nanocrystals. *Angew. Chem. Int. Ed.*, **2017**, *56*(41):12471-12475
- [93] Yang B, Hong F, Chen J S, Tang Y X, Yang L, Sang Y B, Xia X S, Guo J W, He H X, Yang S Q, Deng W Q, Han K L. Colloidal Synthesis and Charge-Carrier Dynamics of $\text{Cs}_2\text{AgSb}_{1-y}\text{Bi}_y\text{X}_6$ ($\text{X}: \text{Br}, \text{Cl}; 0 \leq y \leq 1$) Double Perovskite Nanocrystals. *Angew. Chem. Int. Ed.*, **2019**, *58*(8):2278-2283
- [94] Yang B, Han K L. Ultrafast Dynamics of Self-Trapped Excitons in Lead-Free Perovskite Nanocrystals. *J. Phys. Chem. Lett.*, **2021**, *12*(34):8256-8262
- [95] Cheng X H, Jing L, Yuan Y, Du S J, Yao Q, Zhang J, Ding J X, Zhou T L. Centimeter-Size Square 2D Layered Pb-Free Hybrid Perovskite Single Crystal $(\text{CH}_3\text{NH}_3)_2\text{MnCl}_4$ for Red Photoluminescence. *CrystEngComm*, **2019**, *21*(27):4085-4091
- [96] Xu L J, Lin H R, Lee S J, Zhou C K, Worku M, Chaaban M, He Q Q, Plaviak A, Lin X S, Chen B H, Du M H, Ma B W. OD and 2D: The Cases of Phenylethylammonium Tin Bromide Hybrids. *Chem. Mater.*, **2020**, *32*(11):4692-4698
- [97] Wu Y, Shi C M, Xu L J, Yang M, Chen Z N. Reversible Luminescent Vapochromism of a Zero-Dimensional Sb^{3+} -Doped Organic-Inorganic Hybrid. *J. Phys. Chem. Lett.*, **2021**, *12*(13):3288-3294
- [98] Zhang Y, Yang C, Feng J, Wang N, Li Q, Guo F W, Wang J, Xu D S. High-Efficiency Histamine-In-Based Halide Phosphors with Excellent Thermal Stability. *Sci. Sin. Chim.*, **2021**, *51*(7):967-974
- [99] Zhou J, Li M Z, Molokeev M S, Sun J Y, Xu D H, Xia Z G. Tunable Photoluminescence in Sb^{3+} -Doped Zero-Dimensional Hybrid Metal Halides with Intrinsic and Extrinsic Self-Trapped Excitons. *J. Mater. Chem. C*, **2020**, *8*(15):5058-5063
- [100] Li Z Y, Song G M, Li Y, Wang L, Zhou T L, Lin Z S, Xie R J. Realizing Tunable White Light Emission in Lead-Free Indium(III) Bromine Hybrid Single Crystals through Antimony(III) Cation Doping. *J. Phys. Chem. Lett.*, **2020**, *11*(23):10164-10172
- [101] Artem'ev A V, Davydova M P, Berezin A S, Brel V K, Morgalyuk V P, Bagryanskaya I Y, Samsonenko D G. Luminescence of the Mn^{2+} Ion in Non- O_h and T_d Coordination Environments: the Missing Case of Square Pyramid. *Dalton Trans.*, **2019**, *48*(43):16448-16456
- [102] Ba Q K, Jana A, Wang L H, Kim K S. Dual Emission of Water-Stable 2D Organic-Inorganic Halide Perovskites with Mn(II) Dopant. *Adv. Funct. Mater.*, **2019**, *29*(43):1904768
- [103] Cortecchia D, Mroz W, Neutzner S, Borzda T, Folpini G, Brescia R, Petrozza A. Defect Engineering in 2D Perovskite by Mn(II) Doping for Light-Emitting Applications. *Chem.*, **2019**, *5*(8):2146-2158
- [104] Mei Y X, Yu H, Wei Z H, Mei G Q, Cai H. Two Coordinated Geometries of Mn^{2+} Ions in One Single Molecule: Organic-Inorganic Hybrids Constructed with Tris(2-aminoethyl)amine and Manganese Halide and Fluorescent Properties. *Polyhedron*, **2017**, *127*:458-463
- [105] Biswas A, Bakthavatsalam R, Kundu J. Efficient Exciton to Dopant Energy Transfer in Mn^{2+} -Doped $(\text{C}_4\text{H}_9\text{NH}_3)_2\text{PbBr}_4$ Two-Dimensional (2D) Layered Perovskites. *Chem. Mater.*, **2017**, *29*(18):7816-7825
- [106] Sarang S, Delmas W, Naghadeh S B, Cherrette V, Zhang J Z, Ghosh S. Low-Temperature Energy Transfer via Self-Trapped Excitons in Mn^{2+} -Doped 2D Organometal Halide Perovskites. *J. Phys. Chem. Lett.*, **2020**, *11*(24):10368-10374
- [107] Su B B, Molokeev M S, Xia Z G. Unveiling Mn^{2+} Dopant States in Two-Dimensional Halide Perovskite toward Highly Efficient Photoluminescence. *J. Phys. Chem. Lett.*, **2020**, *11*(7):2510-2517
- [108] Yu J C, Kong J T, Hao W, Guo X T, He H J, Leow W R, Liu Z Y,

- Cai P Q, Qian G D, Li S Z, Chen X Y, Chen X D. Broadband Extrinsic Self-Trapped Exciton Emission in Sn-Doped 2D Lead-Halide Perovskites. *Adv. Mater.*, **2019**,*31*(7):e1806385
- [109]Zhou G J, Liu Z Y, Huang J L, Molokeev M S, Xiao Z W, Ma C G, Xia Z G. Unraveling the Near-Unity Narrow-Band Green Emission in Zero-Dimensional Mn²⁺-Based Metal Halides: A Case Study of (C₁₀H₁₆N)₂Zn_{1-x}Mn_xBr₄ Solid Solutions. *J. Phys. Chem. Lett.*, **2020**, *11*(15):5956-5962
- [110]Pan H M, Yang Q L, Xing X X, Li J P, Meng F L, Zhang X, Xiao P C, Yue C Y, Lei X W. Enhancement of the Photoluminescence Efficiency of Hybrid Manganese Halides through Rational Structural Design. *Chem. Commun.*, **2021**,*57*(56):6907-6910
- [111]Ma Y Y, Song Y R, Xu W J, Zhong Q Q, Fu H Q, Liu X L, Yue C Y, Lei X W. Solvent-Free Mechanochemical Syntheses of Microscale Lead-Free Hybrid Manganese Halides as Efficient Green Light Phosphors. *J. Mater. Chem. C*, **2021**,*9*(31):9952-9961
- [112]Li M Z, Li Y W, Molokeev M S, Zhao J, Na G R, Zhang L J, Xia Z G. Halogen Substitution in Zero-Dimensional Mixed Metal Halides toward Photoluminescence Modulation and Enhanced Quantum Yield. *Adv. Opt. Mater.*, **2020**,*8*(16):2000418
- [113]Zhou L, Zhang L, Li H, Shen W, Li M, He R X. Defect Passivation in Air-Stable Tin(IV)-Halide Single Crystal for Emissive Self-Trapped Excitons. *Adv. Funct. Mater.*, **2021**,*31*(51):2108561
- [114]Wei Q, Chang T, Zeng R S, Cao S, Zhao J L, Han X X, Wang L H, Zou B S. Self-Trapped Exciton Emission in a Zero-Dimensional (TMA)₂SbCl₅·DMF Single Crystal and Molecular Dynamics Simulation of Structural Stability. *J. Phys. Chem. Lett.*, **2021**,*12*(30):7091-7099
- [115]Wu Y Y, Fan W B, Gao Z R, Tang Z, Lei L, Sun X F, Li Y L, Cai H L, Wu X S. New Photoluminescence Hybrid Perovskites with Ultrahigh Photoluminescence Quantum Yield and Ultrahigh Thermostability Temperature up to 600 K. *Nano Energy*, **2020**,*77*:105170